NASA CR-134990
SRD-76-021

IMPROVED TOUGHNESS OF SILICON CARBIDE

by John A. Palm

GENERAL ELECTRIC COMPANY
CORPORATE RESEARCH AND DEVELOPMENT

prepared for

NATIONAL AERONAUTICS AND SPACE ADMINISTRATION

NASA Lewis Research Center
Contract NAS3-17832

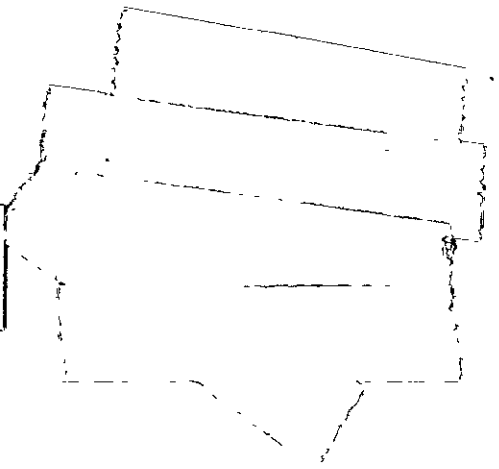

FINAL REPORT

January 1976

1 Report No.	2. Government Accession No.	3 Recipient's Catalog No
NASA CR-134990		

4 Title and Subtitle	5 Report Date
IMPROVED TOUGHNESS OF SILICON CARBIDE	January 1976
	6 Performing Organization Code

7. Author(s)	8 Performing Organization Report No.
John A. Palm	SRD-76-021
	10 Work Unit No. YOG 5724
9 Performing Organization Name and Address General Electric Company Corporate Research and Development P.O. Box 8 Schenectady, New York 12301	11 Contract or Grant No. NAS3-17832
	13 Type of Report and Period Covered Final Report
12. Sponsoring Agency Name and Address National Aeronautics and Space Administration Washington, D.C. 20546	14. Sponsoring Agency Code

15. Supplementary Notes

Project Manager, James R. Johnston
Materials and Structures Division
NASA Lewis Research Center, Cleveland, Ohio

16. Abstract

Impact energy absorbing layers (EALs) comprised of partially densified silicon carbide were formed in situ on fully sinterable silicon carbide substrates. After final sintering, duplex silicon carbide structures resulted which were comprised of a fully sintered, high density silicon carbide substrate or core, overlayed with an EAL of partially sintered silicon carbide integrally bonded to its core member. Thermal cycling tests proved such structures to be moderately resistant to oxidation and highly resistant to thermal shock stresses. The strength of the developed structures in some cases exceeded but essentially it remained the same as the fully sintered silicon carbide without the EAL. Ballistic impact tests indicated that substantial improvements in the toughness of sintered silicon carbide were achieved by the use of the partially densified silicon carbide EALs.

17. Key Words (Suggested by Author(s))	18 Distribution Statement
Silicon Carbide Energy Absorbing Surfaces Impact Resistance Pressureless Sintering	Unclassified - unlimited

19 Security Classif. (of this report)	20 Security Classif. (of this page)	:
Unclassified	Unclassified	

FOREWORD

The research and development work described in this report was carried out within the Ceramics Branch of the Physical Chemistry Laboratory, at the General Electric Corporate Research and Development Center. It was conducted under National Aeronautics and Space Administration Contract No. NAS3-17832. Mr. James R. Johnston of the National Aeronautics and Space Administration Lewis Research Center was the Contract Manager. Mr. John A. Palm was the principal investigator and Dr. R. J. Charles, Manager of the Ceramics Branch, was Program Manager and Technical Director.

The author acknowledges with thanks the technical assistance provided by W. J. Dondalski, C. W. Krystyniak, J. W. Szymaszek and the testing and determination of mechanical properties by R. F. Berning and associates. Discussions with Dr. R. J. Charles, Dr. S. Prochazka, Dr. R. A. Giddings, and Dr. C. A. Johnson were helpful and appreciated.

TABLE OF CONTENTS

LIST OF FIGURES

LIST OF FIGURES (CONTINUED)

LIST OF FIGURES (CONTINUED)

LIST OF TABLES

ABSTRACT

Impact energy absorbing layers (EALs) comprised of partially densified silicon carbide were formed *in situ* on fully sinterable silicon carbide substrates. After final sintering, duplex silicon carbide structures resulted which were comprised of a fully sintered, high density silicon carbide substrate or core, overlayed with an EAL of partially sintered silicon carbide integrally bonded to its core member. Thermal cycling tests proved such structures to be moderately resistant to oxidation and highly resistant to thermal shock stresses. The strength of the developed structures in some cases exceeded but essentially it remained the same as the fully sintered silicon carbide without the EAL. Ballistic impact tests indicated that substantial improvements in the toughness of sintered silicon carbide were achieved by the use of the partially densified silicon carbide EALs.

I. SUMMARY

A single type of silicon carbide (SiC)-energy absorbing layer (EAL) system was examined with the objective of developing the material system and forming procedures necessary to significantly improve the impact toughness of SiC ceramic.

Duplex structures comprised of a dense SiC ceramic core or substrate and a porous SiC surface layer or EAL were formed by both die-pressing and a combination of die-pressing (the core) and dip-coating (the EAL). In each instance final consolidation was carried out in a single step sintering process.

Charpy impact-test bars were made by die-pressing using a fully sinterable boron-doped SiC powder as the core between two opposing and thin layers of a SiC powder that sintered to considerably less than full density. The wide scatter in the Charpy impact test data led to inconclusive results. It did appear, however, that there were no substantial differences in the Charpy impact values between specimens of the same configuration and composition when measured at both room and elevated temperatures.

Three-point bend-test bars were made by the same die-pressing technique as was used for the Charpy impact-test bars. This resulted in the same dense core with a two opposing EAL configuration. Bend-test bars of this configuration were tested in three-point bending to show that the processing steps employed in the application of the EALs by die-pressing and sintering do not cause any weakening of the core member of the structure. Additional bend tests conducted at both room and elevated temperatures resulted in essentially the same values of bend strength at the two temperatures. It was further noted that the quite narrow scatter band in the results of any one test group of the same composition and temperature seemed to suggest that the scatter in flaw size had been narrowed by the use of an EAL of this type, resulting in a more uniform strength from test bar to test bar.

Three-point bend tests conducted on groups of six specimens, each with EALs having different levels of boron doping indicated that those having no boron in their EALs were incrementally weaker at room temperature and incrementally stronger at elevated temperature than those specimens fabricated with small additions of boron to the EAL composition.

Ballistic impact test plates were made by the die-pressing technique described above. The room temperature ballistic impact resistance of these specimens was substantially improved over those test pieces not protected by the SiC energy absorbing layer.

Thermal cycling test wedges were fabricated by die-pressing the core body and partially sintering it prior to dip-coating it with the SiC EAL. A final sintering procedure completed the fabrication of the thermal cycling test wedges equipped with their EALs. Excellent thermal shock resistance was demonstrated, and very small weight changes over the test period indicated little, if any, chemical interaction of the test specimens with the test equipment.

II. INTRODUCTION

Brittle materials are particularly subject to stress conditions that exceed critical values, even though they may occur in very local regions and for extremely short periods of time.

The contemplated use in advanced turbines of materials such as SiC and silicon nitride (Si_3N_4) requires that significant improvements be made in the toughness of these materials - toughness being a measure of their resistance to fracture under conditions of mechanical shock loading. The type of shock loading anticipated is that which arises during collision of a foreign object with a structural component when significant relative velocity difference exists between these bodies just prior to impact. In spite of their many desirable features, including excellent oxidation resistance, these two candidate materials exhibit strengths which result in only marginal resistance to damage by impact. Using the basic approach of improving the impact strength of Si_3N_4 by maximizing its fracture stress through the elimination of strength limiting flaws, T. R. Wright and D. E. Niesz observed little or no improvement in impact strength over previously developed materials.[1]

Irrespective of the mechanisms which generate critical stresses in samples of the above materials, the damage which results is invariably of a type which originates and initiates at the free surfaces of the specimen. This damage may be localized, such as that occurring at the point of contact of an impacting body, or it may be sufficiently extensive to cause complete rupture of the body. High temperature structural ceramics are in this regard similar to any other ceramic in that their toughness or strength is primarily a surface-dependent property.

A desirable goal, therefore, is the development of a ceramic that maintains strength and rigidity and at the same time exhibits improved resistance to local and catastrophic failure under shock loading conditions. A promising approach for improving the impact toughness of a high-strength refractory material is to provide a surface that would (a) absorb impact energy by both elastic and inelastic processes; (b) prolong the impact time to decrease the maximum, momentary loads imparted to the substrate; and (c) redistribute the applied load over a larger area, and thereby decrease the applied contact stress. These surfaces could be essentially non-load-bearing structures which are crushable or deformable and which are inserted between the impacting body and the load-bearing structure. H. P. Kirchner and J. Seretsky have investigated surface treatments resulting in energy absorbing

layers and have observed improvements in impact resistance at room and elevated temperatures.[2] Other approaches under recent or current investigation for improving impact toughness include the incorporation of fibrous additions into the body of the ceramic to improve its resistance to crack propagation,[3] and the formation of ceramic surfaces put under a compressive stress which serves to increase the shock loading required for existing surface flaws to act as crack generators.[4]

In a program prior to this one and conducted by this Laboratory, surface layers were applied to hot-pressed SiC by two methods[5] namely, the chemical alteration of the SiC surface and the formation of porous layers on the SiC surface. The results of that investigation showed that the application of energy absorbing layers by those methods, onto the surface of fully dense SiC, damaged the surface of the SiC to such a degree that serious degradations in the strength of the SiC resulted.

This report describes the results of an investigation designed to improve the impact toughness of SiC by developing processes by which EALs of SiC would be applied to the base SiC or substrate in a single-step consolidation process to produce a graded density structure, the surface structure being porous as compared to the dense strong SiC substrate. It was expected that by utilizing SiC as the EAL material, additional benefits would accrue. The problems of chemical and physical compatability generally associated with the use of chemically dissimilar compounds in the same material system, in the same high temperature and reactive environments could probably be avoided. Additionally, it was hoped that the EAL-forming process would not result in any degradation in strength of the substrate silicon carbide.

The approach used was to employ the use of fully sinterable SiC powders[6] for the formation of the base or load-bearing SiC and a less sinterable SiC powder to form the EAL. The duplex structures were to be fabricated by die-pressing and sintering, and by die-pressing the core or base SiC, partially sintering it to give it some strength and applying the EALs by dip-coating, drying and fully sintering the completed article.

In addition to Charpy impact test determinations, an introduction was made into the study of the ballistic impact resistance of these materials.

III. MATERIALS AND PROCEDURES

A. MATERIALS AND TEST SPECIMEN FABRICATION

Sinterable SiC powders synthesized according to S. Prochazka's specifications[6] were purchased from PPG Industries Inc. These were submicron-particle size SiC powders containing small additions (~0.4%) boron and up to 1.0% free carbon. These powders were used to fabricate the dense core or substrate bodies.

The less or not fully sinterable SiC powders for use in the formation of the EALs were formulated with varying amounts of boron (0-1.0%), 0.7% free carbon and in-house synthesized SiC powder.

Test bars for Charpy impact and three-point bend tests were fabricated by die-pressing at 40 MN/m^2. The die cavity in each instance was filled in three layers resulting in a pressed bar comprised of a center section or core of the fully sinterable SiC powder and two thin layers forming EALs on two opposing faces of the center section. The dies were made so that after sintering, the final size of the resulting bars was close to the required dimensions. Final or complete sintering in all cases was carried out in a flowing argon atmosphere at 2050°C with a 15 minute hold period at temperature. Ballistic impact test targets were also made by die-pressing and sintering as described above. Early test targets were fabricated close to 5.08 cm x 5.08 cm in cross section. Thicknesses were in the order of 1.27 cm but varied considerably depending on the core and EAL thicknesses under consideration at the time. Later in the program, ballistic test samples were fabricated in the 5.08 cm x 5.08 cm size and cut into six pieces, each approximately 2.54 cm x 1.67 cm.

Thermal cycling test specimens without EALs were fabricated by die-pressing the fully sinterable SiC powder using a special die-set designed and built for that purpose. They were sintered and densified at 2050°C as described above. Thermal cycling test bars equipped with EALs were made by die-pressing the core body as described above. It was then partially sintered at 1800°C for 15 minutes in a flowing argon atmosphere. It was then dip-coated, using a SiC EAL slip. After slow drying at 110°C for 2-3 days it was final-sintered at 2050°C according to the standard schedule.

The erosion test bars fabricated for testing and evaluation by the NASA-Lewis Research Center were made by the same procedures described above for the thermal cycling test specimens, except

that a rectangular shaped die-set 15.24 cm x 3.81 cm in cross-section was used. The partially sintered blank was then sliced to size before the EAL was applied and final sintered.

Figure 1 is a composite photograph at 1.3X magnification showing samples of all of the EAL-equipped articles described above. From top left and proceeding clockwise they are: an erosion test bar, Charpy impact test bar, bend-test bar, thermal cycling test wedge and a ballistic test plate.

B. TEST PROCEDURES

1. Three-Point Bend Testing

Bend-test specimens having dimensions close to 5.08 mm x 2.54 mm x 45.0 mm long were loaded in three-point flexure with a 38.1 mm span. Short time bend tests were run at room temperature and at 1325°C using an Instron Universal Test machine. No less than three samples were tested for any single test condition or specimen configuration. In most cases six samples were tested.

2. Charpy Impact Testing

Charpy impact test specimens were fabricated as close to the required 6.4 mm x 6.4 mm cross section as possible according to the technique described in the Materials and Test Specimen Fabrication section of this report. Small oversize dimensions were corrected by careful shaping with a fine diamond hone. The tests were conducted on unnotched bars using a Satec Systems Inc. BLI Impact Tester having a basic capacity of 2.72 Joules. It was equipped with interchangeable .45 and .91 Kg strikers. Six tests were made for each specimen and configuration studied, at room temperature and at 1325°C. As described in detail in a report [5] on another program, a high-temperature Charpy impact test equipment was assembled using hydrogen-oxygen heating to bring the Charpy bar quickly to the test temperature (1350°C). Rapid determinations were obtained with this test procedure. The uniformity of bar temperature at 1325°C was measured. The temperature difference between the hottest and "coldest" section of the bar was found to be about 10°C, a variation of less than 1%. Temperatures were measured by optical pyrometer and with a thermocouple placed in a hole drilled from one end of the bar to its center. Temperature measurements were cross-calibrated between the two techniques to factor out effects of emmissivity. Figure 2 shows the high-temperature assembly in operation with a standard unnotched SiC bar in place.

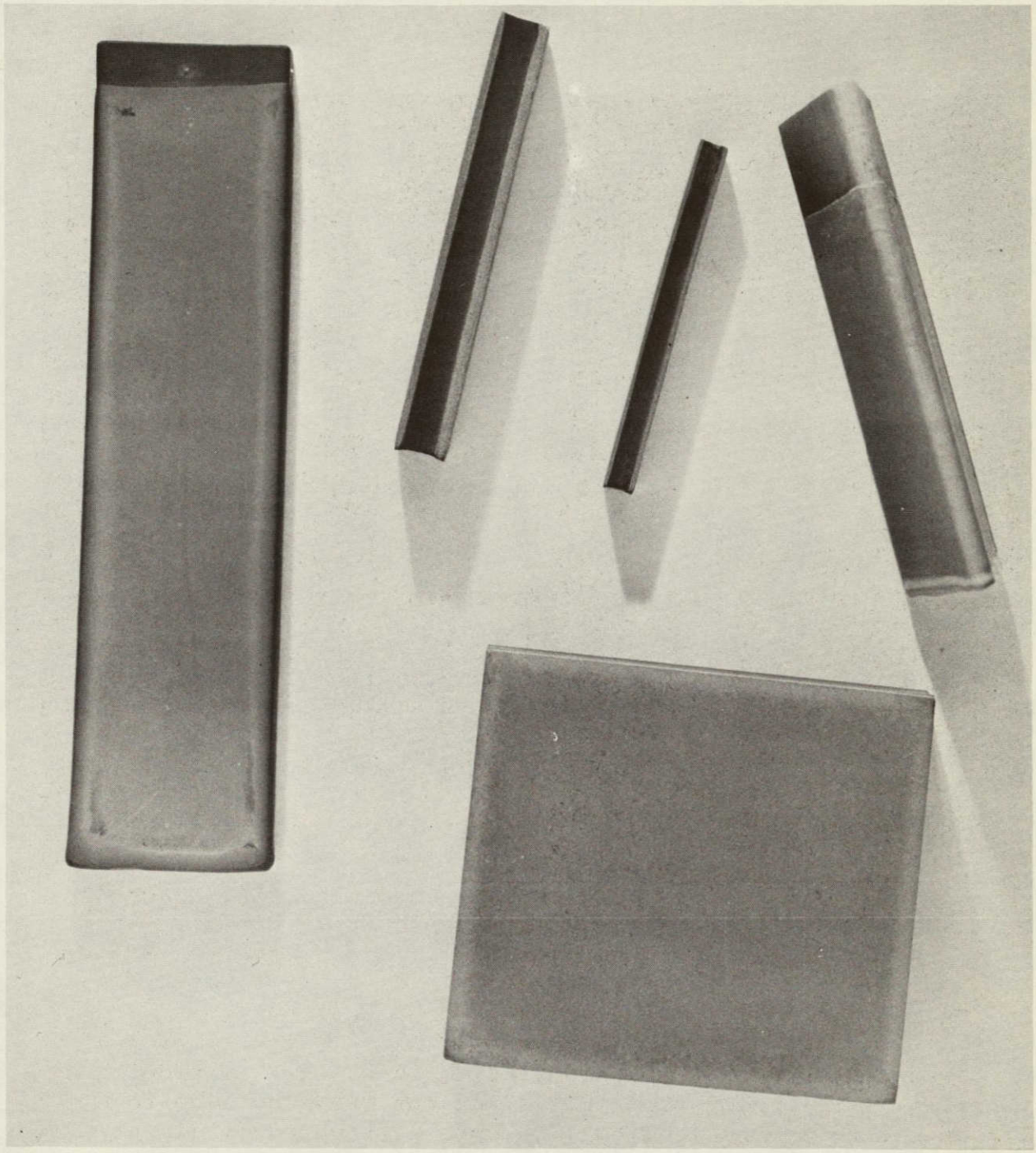

Figure 1. Composite of Samples of Various EAL-Equipped Articles (1.3X)

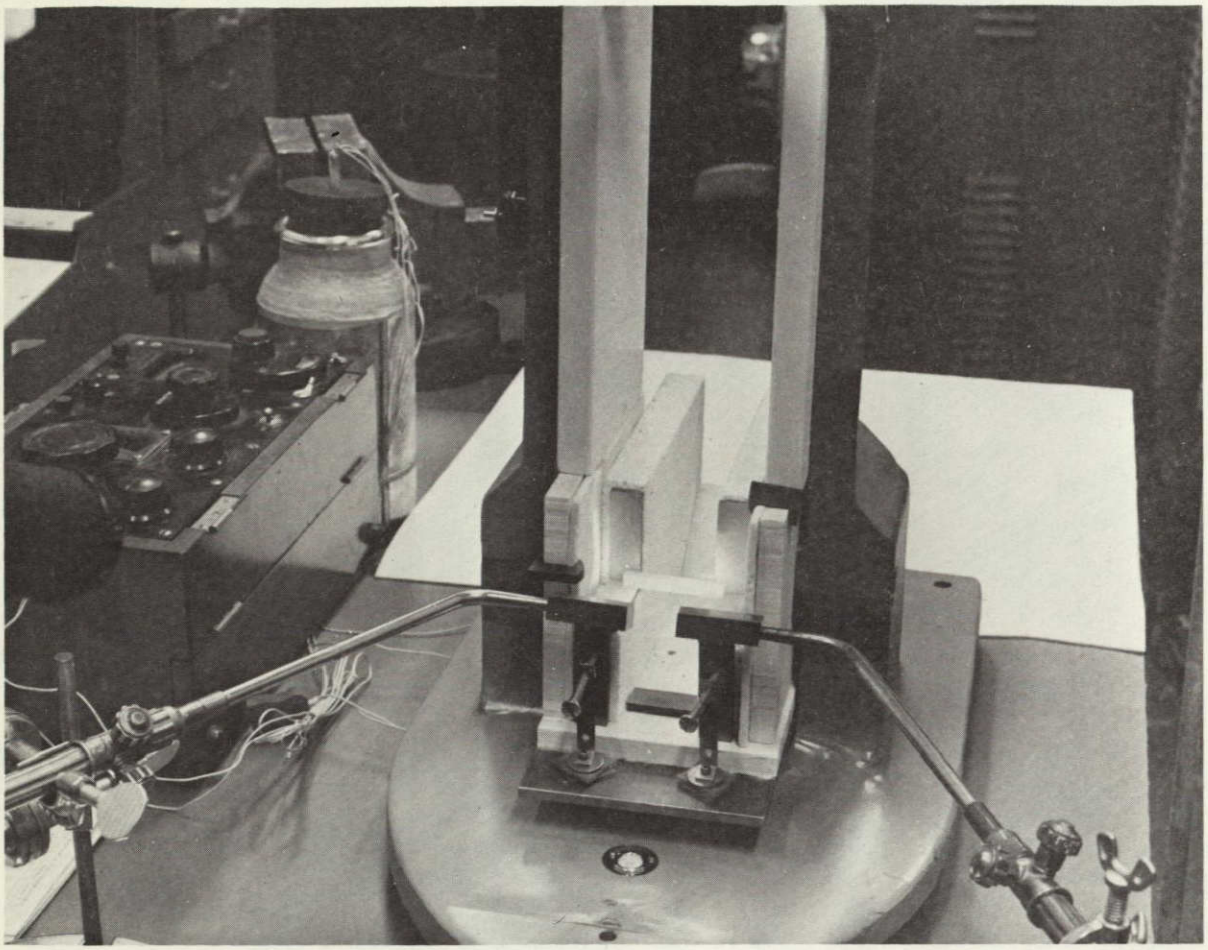

Figure 2. Charpy Impact Tester Assembled for Impact Determinations at 1325°C

3. Thermal Cycling Testing

Wedge shaped test specimens 64 mm long, 25.4 mm wide, and tapering in thickness from 12.7 mm at the trailing edge to a 1.6 mm radius at the leading edge were fabricated by die-pressing as described in another section of this report. EALs were applied by dip-coating the partially sintered wedge, and final consolidation of core and EAL was accomplished in a second sintering at 2050°C in argon. The specimens were subjected to 100 thermal cycles. During each cycle the specimens were heated by a mixture of air and natural gas combustion products to an equilibrium temperature of 1325°C at which temperature they were held for one hour, followed by rapid cooling in an air blast to room temperature. The test samples were examined every 20 cycles for evidence of cracking, spalling and any other sign of thermal shock failure.

Weights and dimensions of the test bars were also measured during the 20 cycle examination periods.

The thermal cycling test equipment was designed and constructed to meet, or very closely meet, the test requirements. Figure 3 is a shop print of the equipment. It featured an air cylinder actuated by a timer, which moved the test bars into and out of the hot gas environment. The original design employed a camera to monitor the condition of the test bars during the cool-down portion of the cycle. It became clear early in the testing program that a camera was not required for failure record purposes. The quality of the materials investigated was such that no failures detectable by the camera system occurred during the 100-cycle test period. Figure 4 shows a portion of the test equipment with a fixture containing four test bars a few seconds after removal from the furnace and about to be quenched. A longer range view showing most of the equipment is shown in Figure 5.

4. Ballistic Impact Testing

The ballistic test equipment was comprised of a Benjamin air rifle rigidly fixed on a metal I-beam. It was used to fire a 4.49 mm diameter hardened steel ball weighing 0.37 g. Helium gas was used to pressurize the gun and fire the pellet. The target was mounted in a vise so that the impact surface was 50 cm from the muzzle of the rifle. A "time trap" consisting of two photo transistor units was mounted between the rifle muzzle and the target and assembled so that the fired pellet would intercept the circuit at two points 15.24 cm apart. The velocity of the pellet was readily computed from the time it took to pass over the measured distance between the two photo transistor gates. Direct readouts in mircoseconds were obtained for the time intervals. The range of impact energies available using the steel pellets described above varied from about 0.25 Joules at a velocity of 36 m/sec to about 8.5 Joules at a velocity of about 214 m/sec. At velocities greater than about 214 m/sec some instability in pellet trajectory developed. A "gun" of improved design allowing velocities in excess of Mach 1 to be generated and with stable pellet flight became available too late in the program to be used.

Figure 6 shows the ballistic test equipment described above.

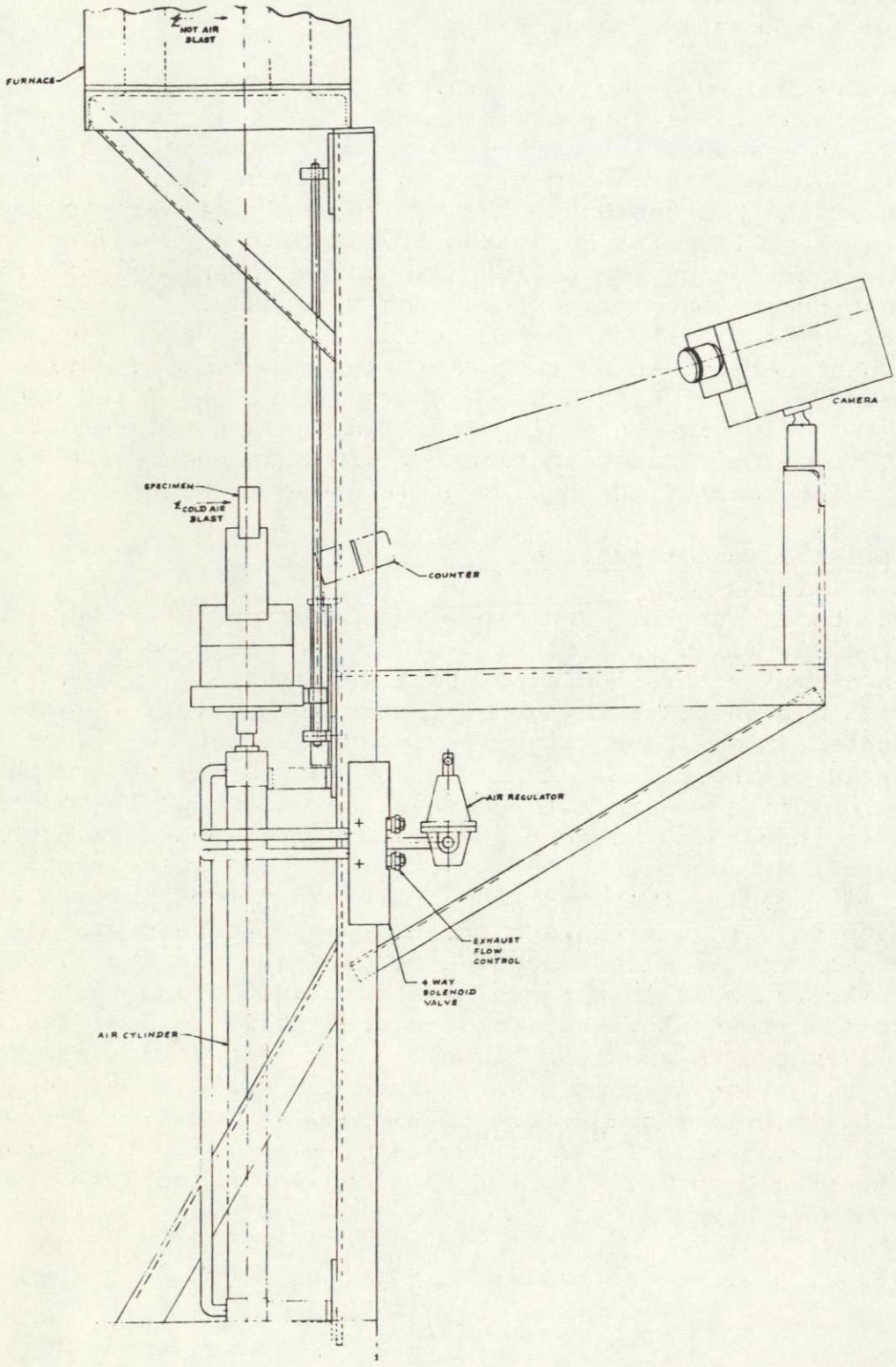

Figure 3. Shop Print of Thermal Cycling Test Equipment

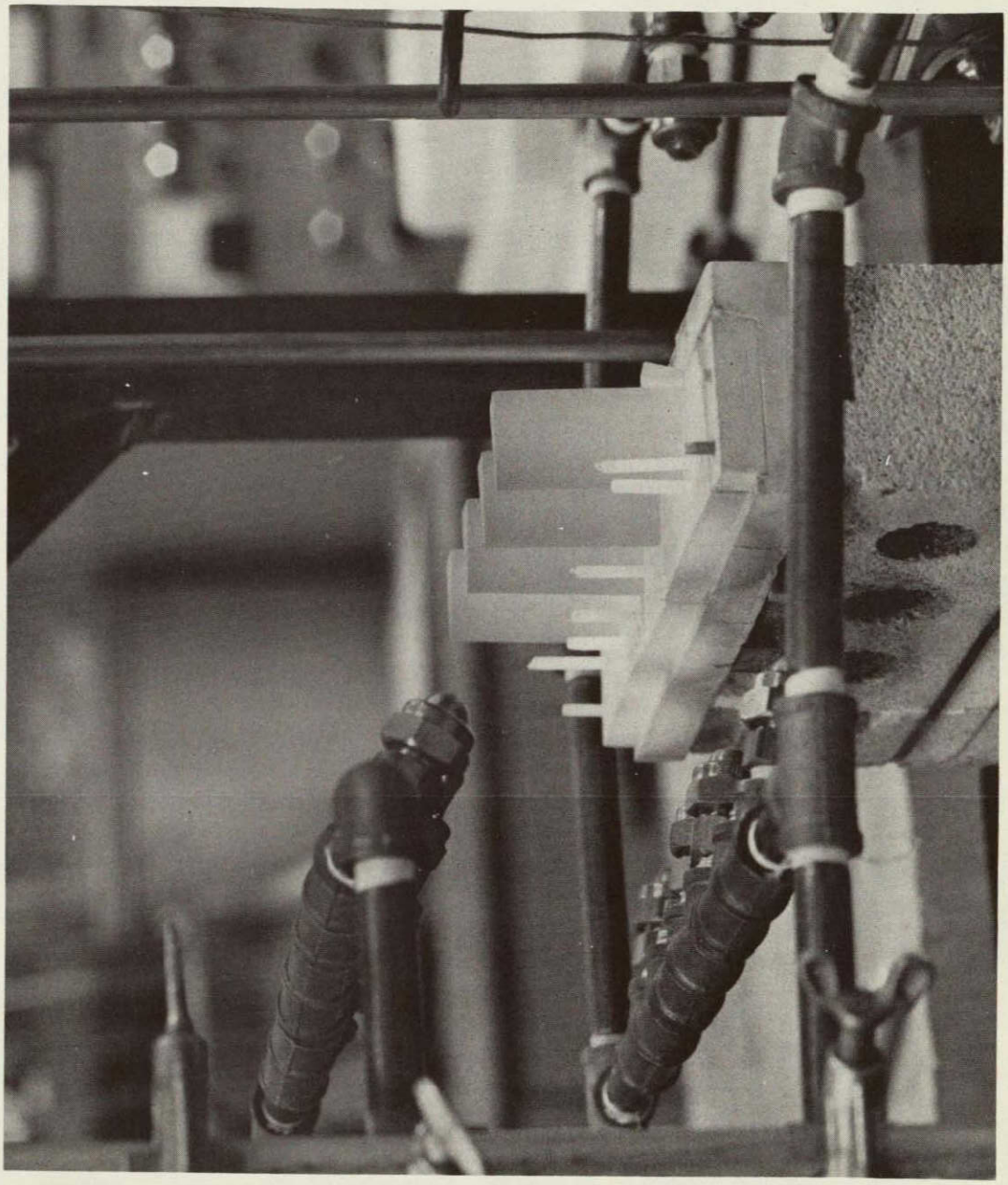

Figure 4. Photograph of Thermal Cycling Specimens in Test Equipment and About to be Quenched

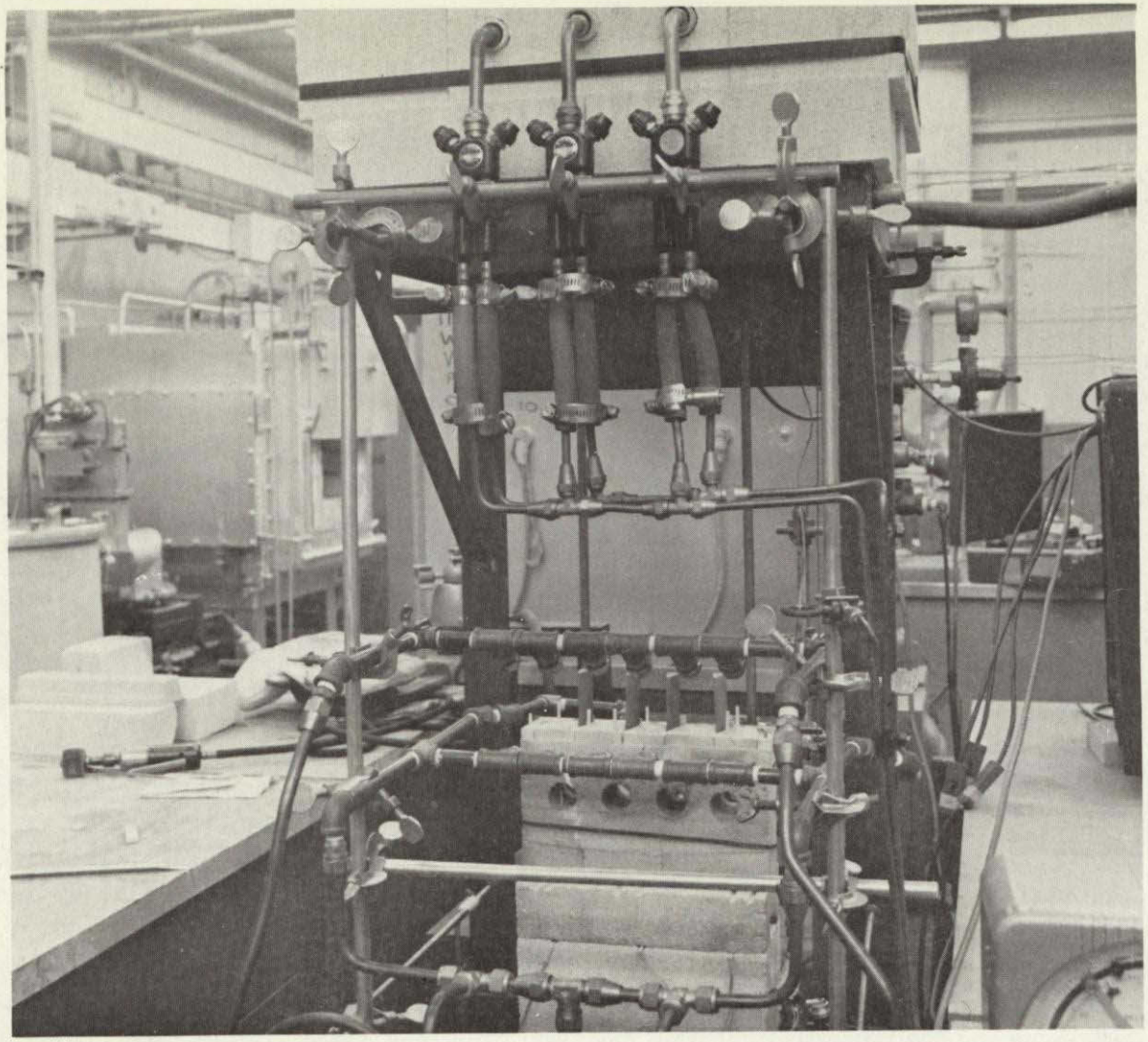

Figure 5. Photograph of Thermal Cycling Test Equipment

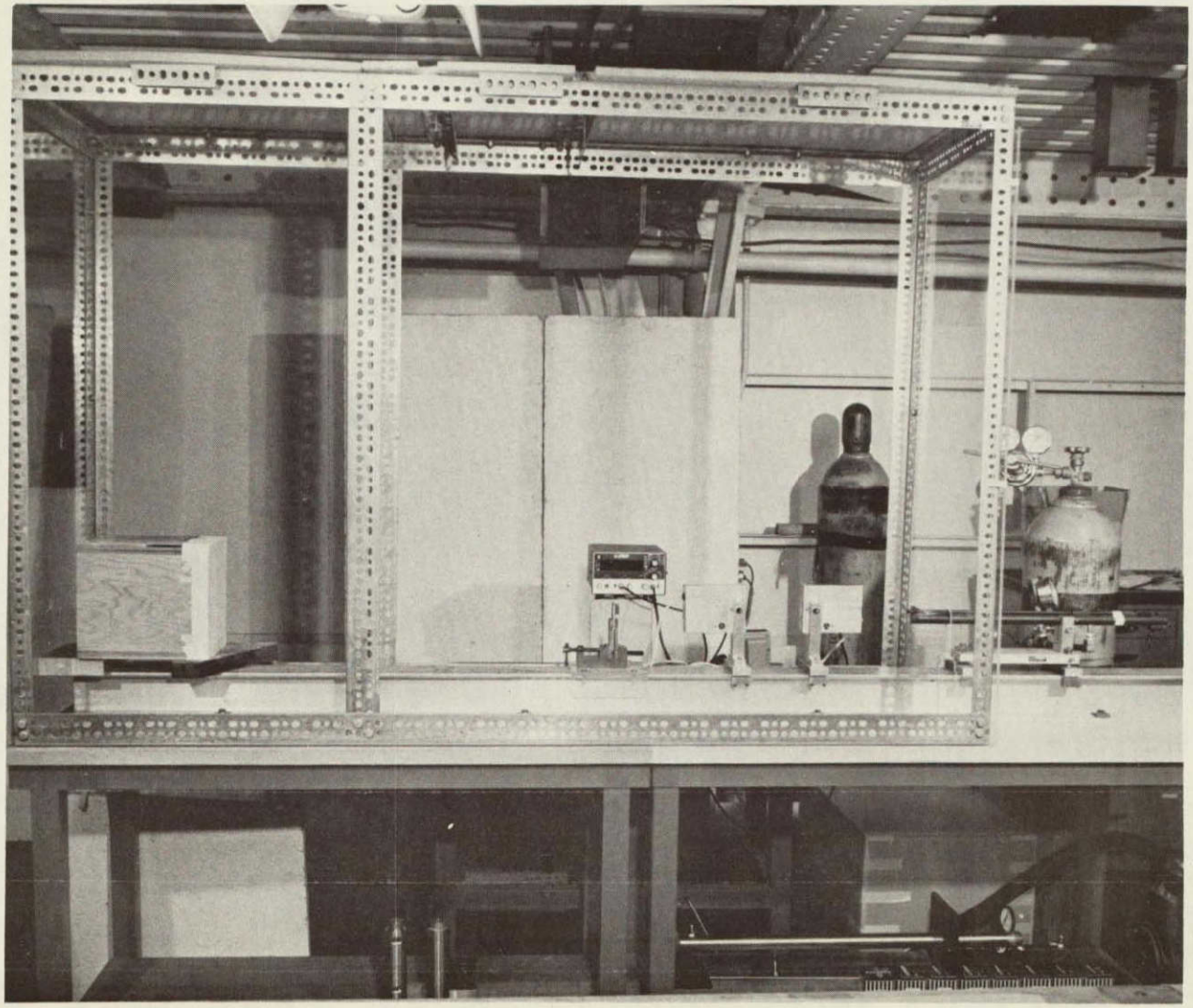

Figure 6. Photograph of Ballistic Test Equipment

IV. RESULTS AND DISCUSSION

A. PROCESSING AND STRUCTURES CHARACTER

1. Die-Pressing

Sample test bars made by the die-pressing technique and with EALs having three different degrees of sintered densities were examined with both optical and electron microscopy. Figures 7, 8, and 9 are optical photographs which show the interface and surface texture between the EAL and dense SiC cores of three samples made with no boron sintering aid in the EAL (Figure 7), 0.5% boron sintering aid in the EAL (Figure 8) and 1.0% boron sintering aid in the EAL (Figure 9). Figures 10, 11, and 12 are scanning electron micrographs of the same three structures, taken at 20X. In Figure 10, a crack in the EAL is apparent, suggesting that some degree of sintering aid could be included in the EAL composition to provide improved bulk integrity. At the same time, too much sintering aid should probably be avoided to prevent the EAL from becoming too dense.

Figures 13, 14, and 15 are SEMs of the same three structures showing the interface and adjoining dense and porous zones at magnifications of 200X and 500X. Excellent detail and viewing of the structural character can be noted.

In Figures 16, 17, and 18 an attempt was made to show in more detail, portions of the dense, transition, and porous zones of the same three structures in which the EALs contained 0%, 0.5% and 1.0% boron sintering aid. In each instance, individual SEMs were taken at 1000X of the three zones and joined together to show the structure changes that occur on traversing from the dense into the porous zones. No large differences can be discerned between the three structures at this high magnification. Differences in EAL density are most readily observed at the lower magnifications.

2. Dip Coating of EALs

Water-based slips for dip-coating were prepared using a non-sinterable SiC powder. SiC concentrations were close to 70% by weight, with a corresponding slip density of close to 2.0 g/cm^3. The slip pH was controlled at close to 10.3 using methyl ammonium hydroxide as the control agent.

Figure 7. Photograph of Interface of SiC Duplex Structure with EAL Containing 0% Boron Sintering Aid (44X)

Figure 8. Photograph of Interface of SiC Duplex Structure with EAL Containing 0.5% Boron Sintering Aid (44X)

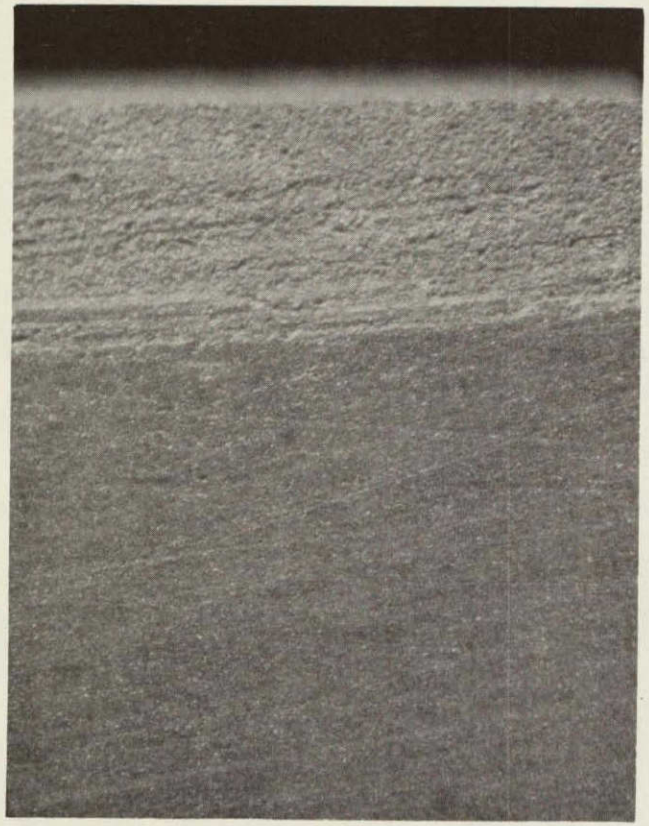

Figure 9. Photograph of Interface of SiC Duplex Structure with EAL Containing 1.0% Boron Sintering Aid (44X)

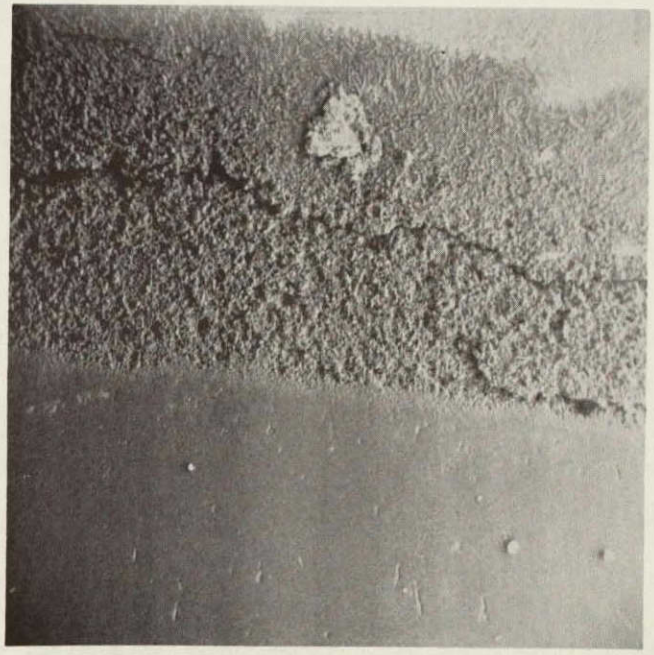

Figure 10. SEM at Interface of SiC Duplex Structure with EAL Containing 0% Boron Sintering Aid (20X)

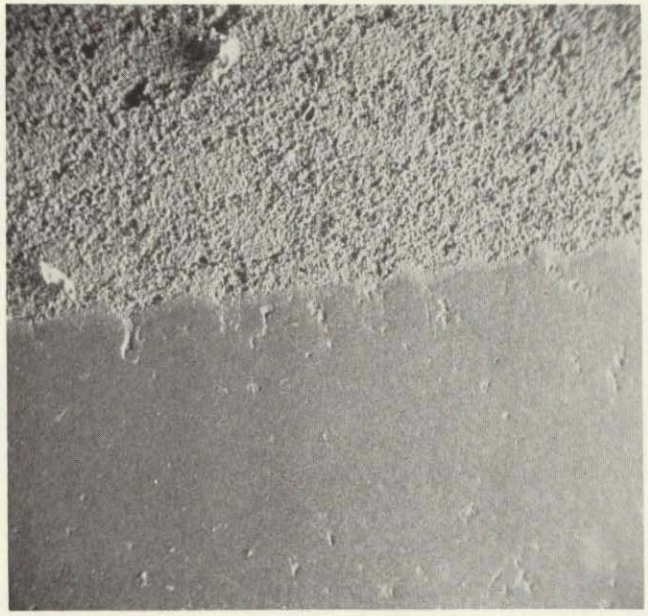

Figure 11. SEM at Interface of SiC Duplex Structure with EAL Containing 0.5% Boron Sintering Aid (20X)

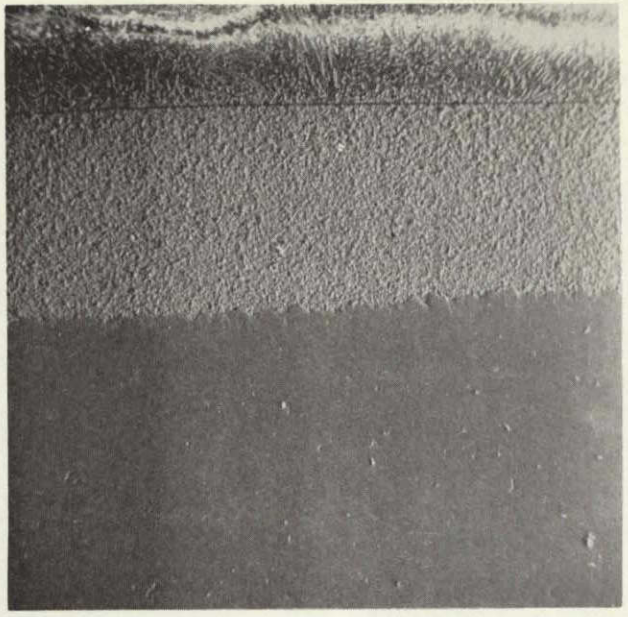

Figure 12. SEM at Interface of SiC Duplex Structure with EAL Containing 1.0% Boron Sintering Aid (20X)

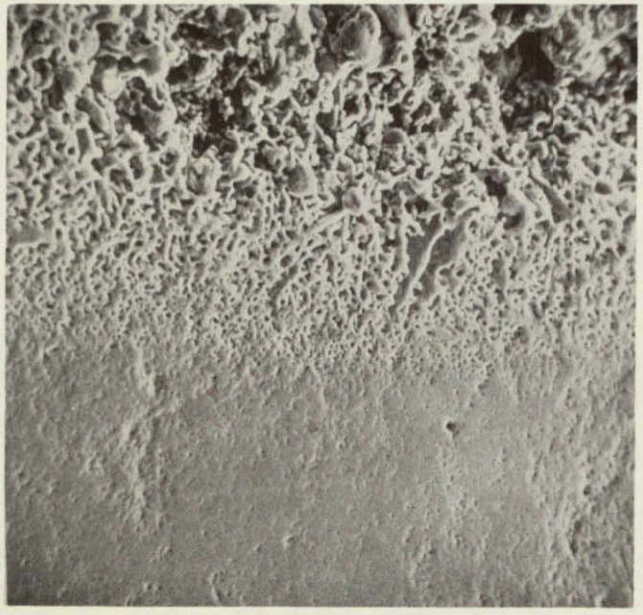

(200X)

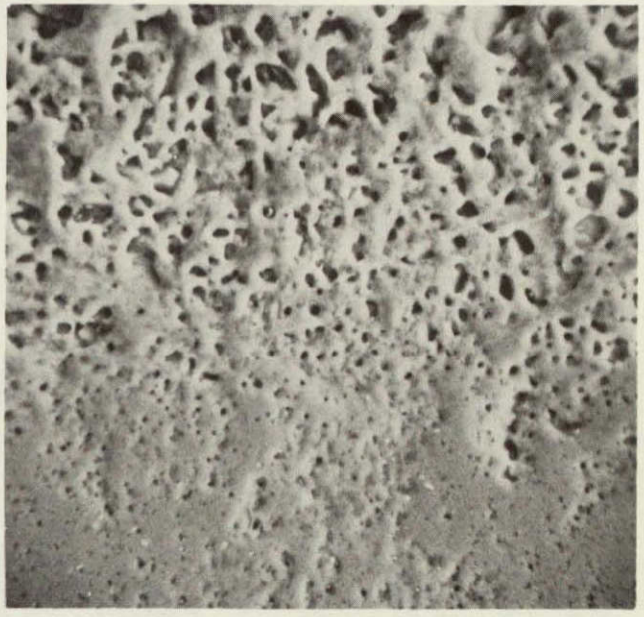

(500X)

Figure 13. SEMs of Interface Between Dense and Porous Sections with EAL Containing 0% Boron Sintering Aid

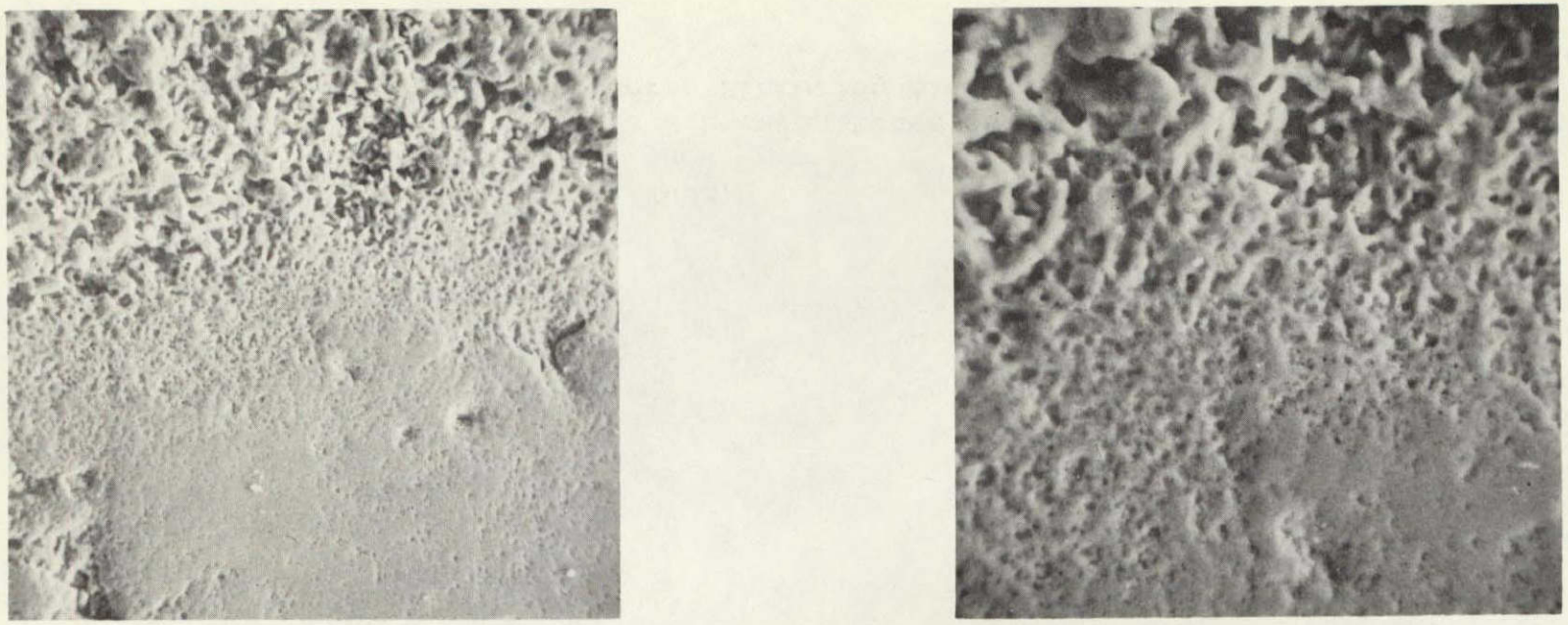

(200X) (500X)

Figure 14. SEMs of Interface Between Dense and Porous Sections with EAL Containing 0.5% Boron Sintering Aid

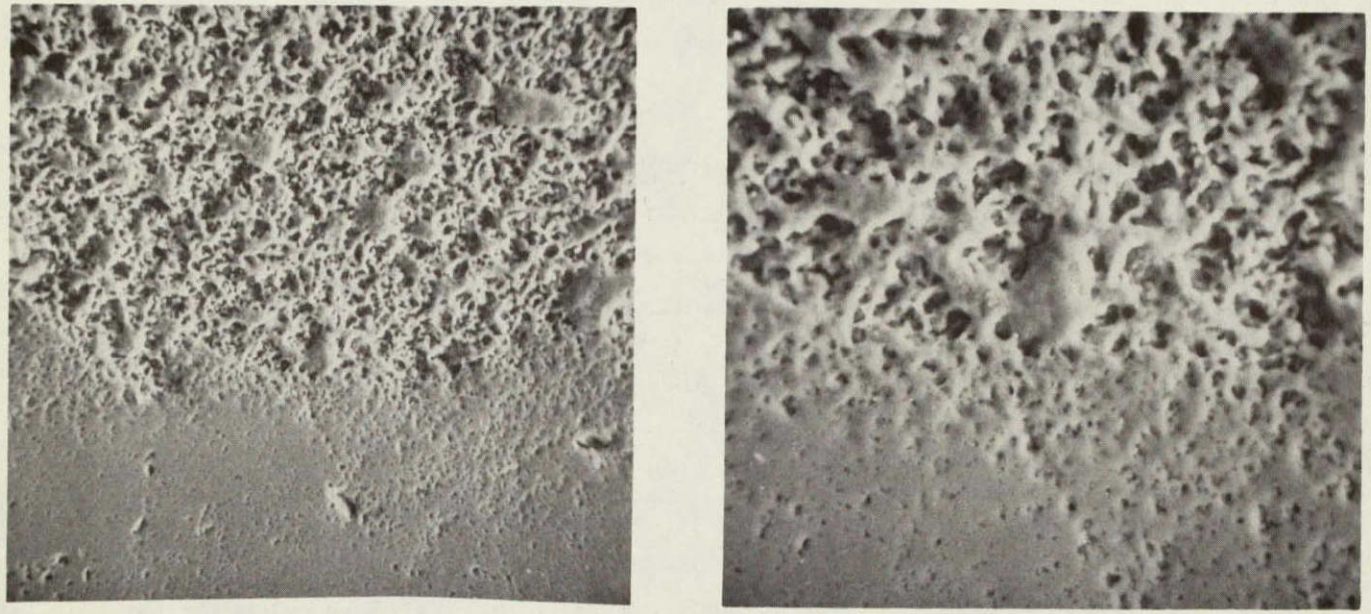

(200X) (500X)

Figure 15. SEMs of Interface Between Dense and Porous Sections with EAL Containing 1.0% Boron Sintering Aid

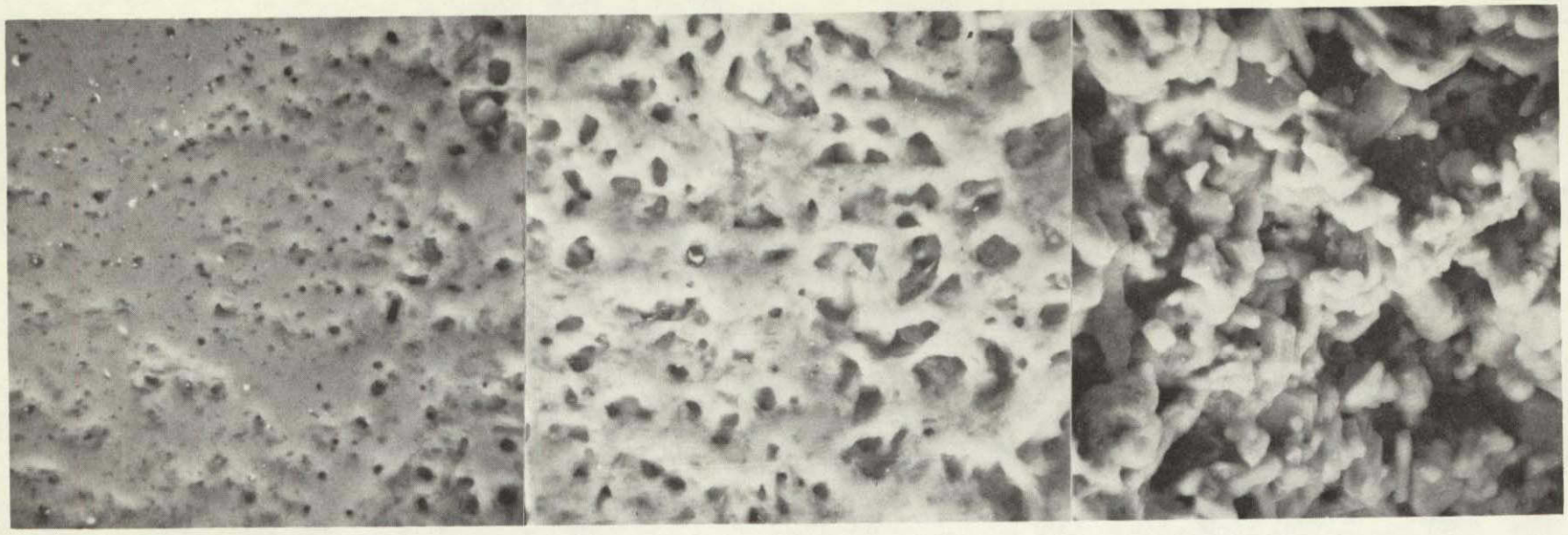

Figure 16. SEM Traverse from Dense Through Porous Zones with EAL Containing 0% Boron Sintering Aid

(930X)

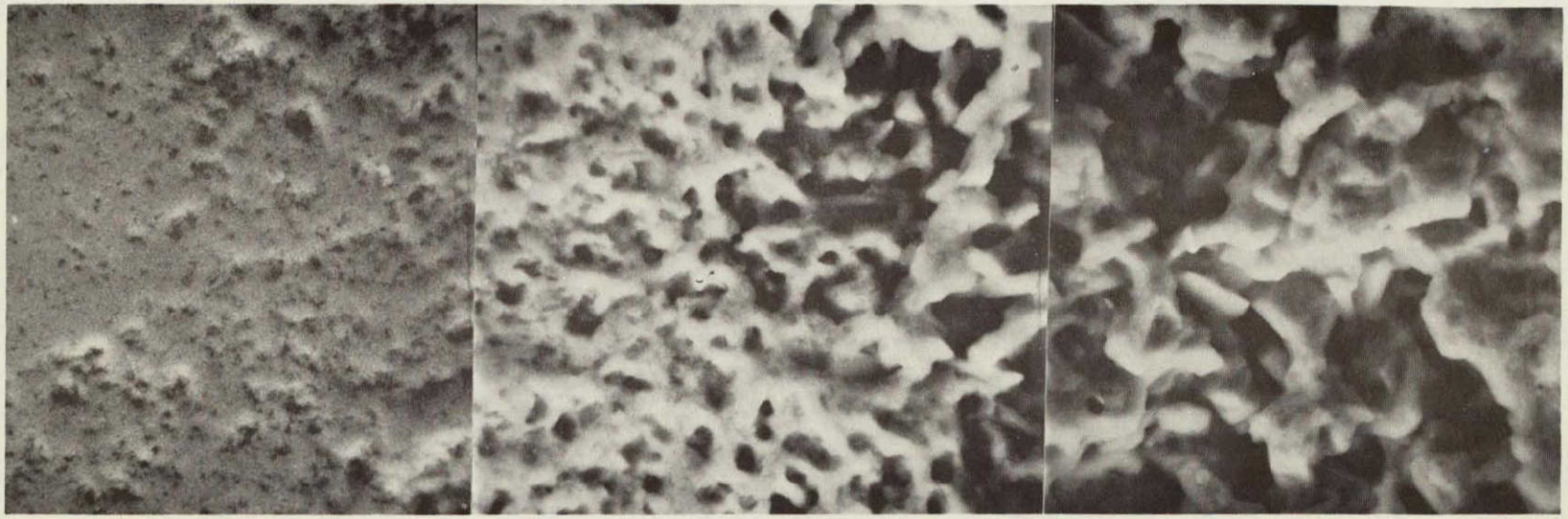

Figure 17. SEM Traverse from Dense Through Porous Zones with EAL Containing 0.5% Boron Sintering Aid (900X)

Figure 18. SEM Traverse from Dense Through Porous Zones with EAL Containing 1.0% Boron Sintering Aid (900X)

Early experiments showed that uniformly thick layers could be applied by dip-coating procedures. Figure 19 shows the cross section at 8X magnification of a 12.7 mm thick layer applied to an experimental iso-pressed core structure. Figure 20 shows an example of pinholes which were observed at the core-EAL interface. It was found that dip-coated EALs applied under conditions in which the slip was thoroughly deaerated and the presintered core was saturated with water eliminated the formation of the voids and pinholes. An apparatus for dip-coating presintered articles was employed to provide a constant rate of immersion and withdrawal during the application of the EAL slip. Typical times for immersing the 10 cm long erosion bars were in the order of 22 secs.

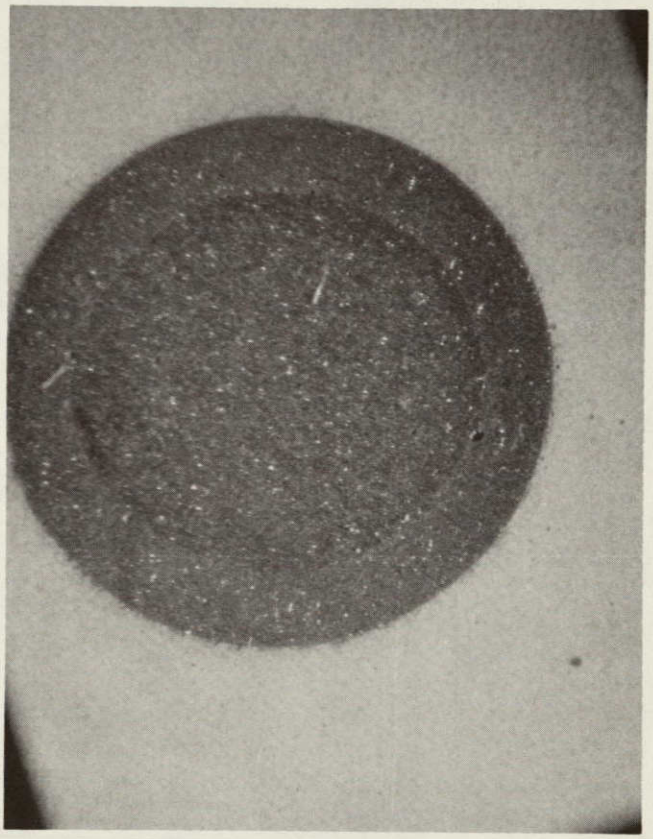

Figure 19. 12.7 mm Thick Dip-coated SiC EAL on Iso-pressed SiC Core (8X)

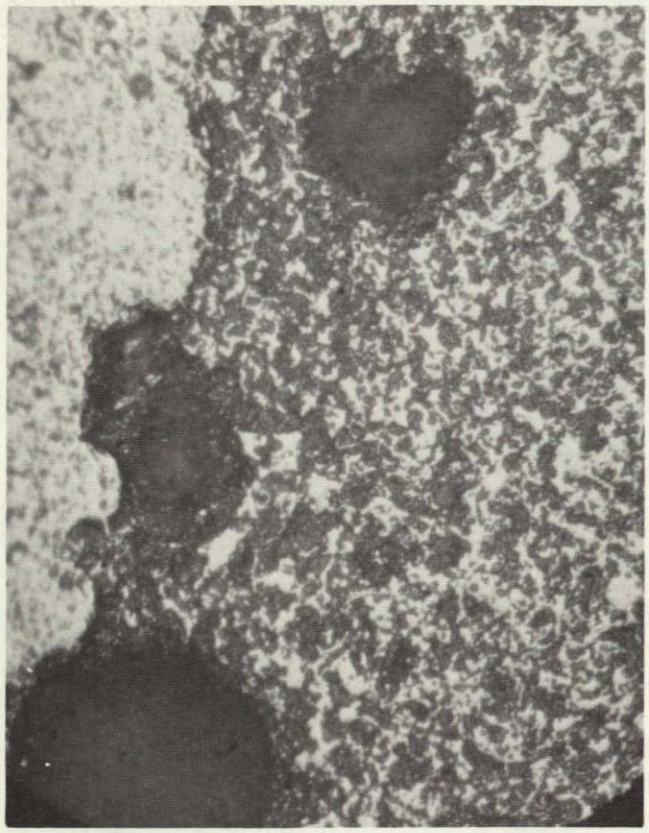

Figure 20. Pinhole Formation at EAL-core Interface (263X)

B. FRACTURE STRENGTH

In many previous attempts to apply EALs of a variety of compositions and structures[5] to fully dense, hot-pressed SiC, it was found that the processing necessary to apply or form an EAL on the surface of the SiC resulted in a serious degradation in strength of the SiC as compared to its value without the EAL.

An experiment was conducted using the die-pressing technique to form EAL core structures by the sintering process to determine if the processing required to form EALs on SiC in that manner had any deleterious effects on the strength of the SiC core material.

Room-temperature bend tests were run on three sets of samples. One set of three specimens were the standard bend-test bars, nominally 5.08 mm x 2.54 mm x 45 mm span. These were lightly ground and polished on all four sides. Edges were sharp and flaw-free as detectable at about 30X magnification. A second set of three samples fabricated with EALs on opposing faces (5.08 mm x 44.5 mm)

had one of the EALs ground off and that face and the two sides were polished to the same finish as the first set. A third set of two samples were equipped with both EALs as applied and the edges were lightly ground and polished. All three sets of samples were fractured in three-point bending and the bend strengths computed using the cross-sectional dimensions of the core or dense member of the structure. Results are shown in Table I.

Table I

THREE-POINT ROOM-TEMPERATURE BEND STRENGTHS ON BARS WITH 0, 1, AND 2 EALs CONTAINING 1.0% B SINTERING AID

Specimen Type and Number	Height (mm)	Width (mm)	Span (mm)	Load to Fracture (N)	Bend Strength (MN/m^2)
Set I					
No EALs					
87A	2.52	4.73	38.1	207	396
87B	2.51	4.73	38.1	146	279
87C	2.52	4.73	38.1	170	326
					av. 334
Set II					
One EAL					
87D	2.57	4.54	38.1	267	508
87E	2.50	4.54	38.1	232	468
87F	2.55	4.54	38.1	227	439
					av. 472
Set III					
Two EALs					
87G	2.78	4.73	38.1	323	506
87H	2.80	4.73	38.1	283	439
					av. 472

These results showed no difference in bend strength between bars having two EALs (Set III) and those that had two EALs but tested with one EAL ground off, with the ground-off face in tension (Set II). Comparing the bend strengths of Sets II and III with Set I, those samples fabricated with no EALs, a 40% increase in bend strength was noted in those samples that were fabricated with two EALs.

From these results it appeared that the processing steps employed in the application of the EALs by die-pressing and sintering do not cause any weakening of the core member of the structure. The 40% increase in bend strengths noted in Sets II and III over Set I may be due either to the protection afforded the core member surface by the EAL or possibly to the added strength provided by the EAL, the thickness of which was not considered in the computation of the bend strength.

The bend strength values obtained on samples in Set I should not be considered as typical of what can be obtained with the sintered SiC. All of the specimens made for Sets I, II, and III were made with the early processing techniques and procedures. More recent results from another program show that with careful and specific precautions, sintered SiC can be made with strengths in excess of 690 MN/m^2.

In another experiment, three-point bend tests were run at room temperature and at 1325°C on three different sets of samples. The purpose of the experiment was to determine the effect on bend strength of EALs containing different levels of boron sintering aid. It had been noted that increasing percentages of boron in the EAL resulted in increasing density of the EAL. All of the specimens had two EALs (on opposing faces of the test bar). Each bar was fabricated with each EAL powder-charge weight of 0.25 g, and a core powder weight of 1.9 g. These weight ratios resulted in a test bar having a core about 2.54 mm in thickness and two EALs each having a thickness of close to 0.762 mm. The widths of all bars were close to 5.33 mm. The results of these tests are shown in Table II. A fourth set of samples without EALs (Group S) was run at the same time. Those results are also shown in Table II.

Those results show a small decrease in bend strength at 1325°C from the room temperature values for Groups B and C. The loss in strength at temperature is a little more (7.5%) for the specimens in Group C as compared to the 4.5% loss experienced by those in Group B. The Group A samples show the opposite trend. Clearly, those samples proved to be stronger at temperature than those tested at room temperature. Indeed, they were consistently better at temperature than any of the other two groups at either room temperature or 1325°C.

The quite narrow scatter band in the results of any one test group and temperature seemed to suggest that the scatter in flaw size had been narrowed, resulting in a more uniform strength from bar to bar.

Table II

ROOM-TEMPERATURE AND 1325°C BEND TESTS ON SPECIMENS
WITH 2 EALs CONTAINING 0, 0.5, and 1.0% BORON SINTERING AID

Specimen Group and Number	Room Temperature Bend Strength (MN/m^2)	1325°C Bend Strength (MN/m^2)
Group S (No EALs)	88A-1 396	88B-1 - Broke in set-up
	88A-2 361	88B-2 374
	88A-3 396	88B-3 347
		88B-4 270
	av. ---------- 370	av. ---------- 330
Group A (0%B)	88C-1 - Broke in set-up	88D-1 425
	88C-2 367	88D-2 407
	88C-3 335	88D-3 403
	88C-4 339	88D-4 394
	88C-5 319	88D-5 406
	88C-6 361	88D-6 394
	av. ---------- 344	av. ---------- 405
Group B (0.5%B)	88E-1 391	88F-1 373
	88E-2 430	88F-2 355
	88E-3 374	88F-3 382
	88E-4 410	88F-4 380
	88E-5 403	88F-5 363
	88E-6 334	88F-6 366
	av. ---------- 390	av. ---------- 370
Group C (1.0%B)	88G-1 397	88H-1 330
	88G-2 364	88H-2 336
	88G-3 369	88H-3 342
	88G-4 394	88H-4 372
	88G-5 386	88H-5 346
	88G-6 367	88H-6 370
	av. ---------- 380	av. ---------- 349

C. CHARPY IMPACT RESISTANCE

Charpy bars fabricated with two EALs on opposing faces and with three different levels of boron sintering aid were subjected to the Charpy impact test using the 1.36 Joule hammer. Tests were run at room temperature and at 1325°C using the two-torch gas-heating system described in the previous section. Each Charpy bar was fabricated with an EAL powder charge weight of 0.78 g and a core powder weight of 6.0 g. These weight ratios resulted in test bars having total cross-sectional dimensions close to the prescribed 6.35 mm x 6.35 mm. The core or strong member of the structure, however, being close to 4.06 mm in thickness resulted in Charpy impact test results which in order to make comparisons with bars having no EALs, had to be described in terms of the elastic energy stored per unit volume. As with the bend test, the purpose of these tests was to determine the effect on impact resistance of EALs containing different levels of boron sintering aid. The results of these tests are shown in Table III.

Because the cross-sectional area of the specimens with EALs (Groups A_c, B_c, and C_c) was nominally 25.8 mm^2 as compared to the 40.3 mm^2 of the specimens without EALs (Group S_c), the average Charpy values in terms of Joules/cm^3 of volume were computed and are shown in Table IV.

The wide scatter of Charpy impact results within certain groups of these tests shown in Table III was disturbing in view of the very consistent results obtained in the bend strength determinations (Table II). Additionally, undetected cracks in the EALs, as shown in Figure 10, could be responsible for some of the low values.

D. BALLISTIC IMPACT RESISTANCE

Because of the wide scatter in the Charpy impact test results and because a ballistic test evaluation was regarded as closely duplicating the impact process that would occur in the intended applications, some preliminary ballistic tests were conducted. A sintered plate close to 5.7 cm x 5.1 cm x 1.4 cm thick was fabricated by the die-pressing technique. EALs containing 1.0% boron sintering aid and close to 1.5 mm thick were formed on the two opposing faces of the plate. The core was about 1.04 cm in thickness. Using an air rifle securely held in a vise, two steel pellets about 4.5 mm in diameter and weighing 0.37 g were fired at the plate. One pellet was fired with an impact velocity of close to 80 m/sec. Its energy of impact was computed to be close to 1.2 J. A second pellet was fired with an impacting energy close to 5.4 J. The plate appeared to survive the less energetic

Table III

ROOM-TEMPERATURE AND 1325°C CHARPY IMPACT TESTS ON SPECIMENS WITH 2 EALs CONTAINING 0, 0.5, AND 1.0% BORON SINTERING AID

Specimen Group and Number	Room Temp. Charpy Impact Strength (J)	1325°C Bend Strength (MN/m^2)	1325°C Charpy Impact Strength (J)
Group S_c (No EALs)			
94A-1	0.190	94B-1	0.082
94A-2	0.177	94B-2	0.154
94A-3	0.177	94B-3	0.150
94A-4	0.204	94B-4	0.171
94A-5	0.169	94B-5	0.068
94A-6	0.194	94B-6	0.068
	av. 0.185		av. 0.116
Group A_c (0%B in EALs)			
94C-1	0.110	94D-1	0.052
94C-2	0.119	94D-2	0.059
94C-3	0.067	94D-3	0.061
94C-4	0.060	94D-4	0.061
94C-5	0.067	94D-5	0.061
94C-6	0.071	94D-6	0.056
	av. 0.083		av. 0.058
Group B_c (0.5%B in EALs)			
94E-1	0.118	94F-1	0.155
94E-2	0.137	94F-2	0.064
94E-3	0.152	94F-3	0.128
94E-4	0.143	94F-4	0.143
94E-5	0.068	94F-5	0.121
94E-6	0.065	94F-6	0.128
	av. 0.114		av. 0.124
Group C_c (1.0%B in EALs)			
94G-1	0.075	94H-1	0.132
94G-2	0.071	94H-2	0.124
94G-3	0.129	94H-3	0.114
94G-4	0.140	94H-4	0.118
94G-5	0.152	94H-5	0.120
94G-6	0.117	94H-6	0.133
	av. 0.114		av. 0.124

Table IV

SUMMARY OF CHARPY TESTS IN TERMS
OF ELASTIC ENERGY STORED PER UNIT VOLUME

	Room Temp. (Joules/cm^3)	1325°C (Joules/cm^3)
Group S_c (no EALs)	0.120	0.076
Group A_c (0% B in EALs)	0.085	0.059
Group B_c (0.5% B in EALs)	0.116	0.126
Group C_c (1.0% B in EALs)	0.116	0.126

impact with the only damage being the formation of a small crater in the surface of the EAL. The 5.4 J impact made a little larger crater, but it also cracked the target through the thickness of the entire plate. Figures 21 and 22 show the impact areas and EAL surface damage of the two shots. A small crack in the EAL can be seen in Figure 21. The beginning of the more catastrophic crack formed at 5.4 J impact energy is readily seen in Figure 22. Another plate having EALs about 1.0 mm thick and with an overall thickness of about 1.1 cm was also ballistically impacted with an impact energy of about 1.22 J. It was broken into two pieces. Figure 23 is a cross-sectional photograph showing the fracture surface in the vicinity of the impact area. It clearly showed the crushing of the EAL that took place right up to the interface of the EAL and the dense core. Also evident is the crack initiation pattern and mirror created as the shock wave proceeded through the dense core material.

With what appeared to be promising results obtained from the initial ballistic tests, it was concluded that under the test conditions used, the EAL was doing what it was intended to do, and that with the ballistic test, differences in impact resistance due to EAL thickness could be measured directly in terms of energy of impact.

A more sophisticated ballistic test equipment was set up. It was comprised of a rigidly fixed Benjamin air rifle that was used to fire a 4.5 mm diameter hardened steel ball weighing 0.37 g. Helium gas was used to pressurize and fire the pellet. The target was mounted in a vise so that the impact surface was 50 cm from the muzzle of the rifle. A "time trap" consisting of two photo transistor units was mounted between the rifle muzzle and the target and assembled so that a pellet would intercept the circuit

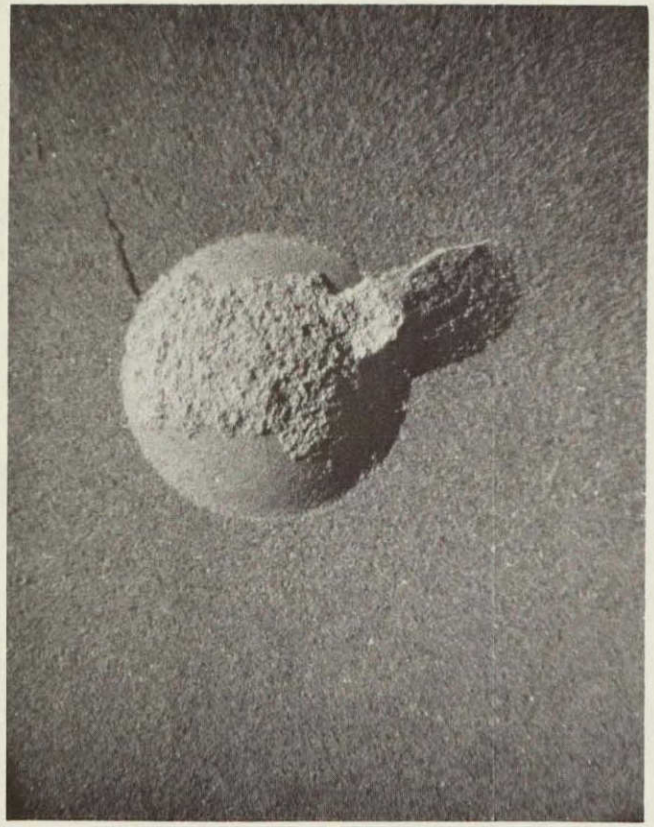

Figure 21. Impact Area and Damage by 1.22 J (Ballistic) on Surface of a 1.5 mm Thick SiC EAL on a SiC Core (17.5X)

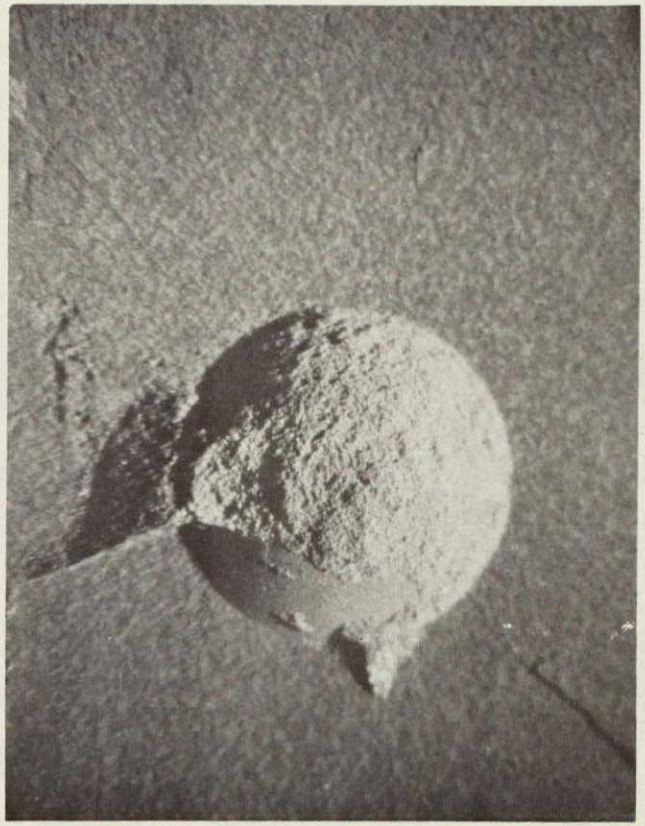

Figure 22. Impact Area and Damage by 5.44 J (Ballistic) on Surface of a 1.5 mm Thick SiC EAL on a SiC Core (17.5X)

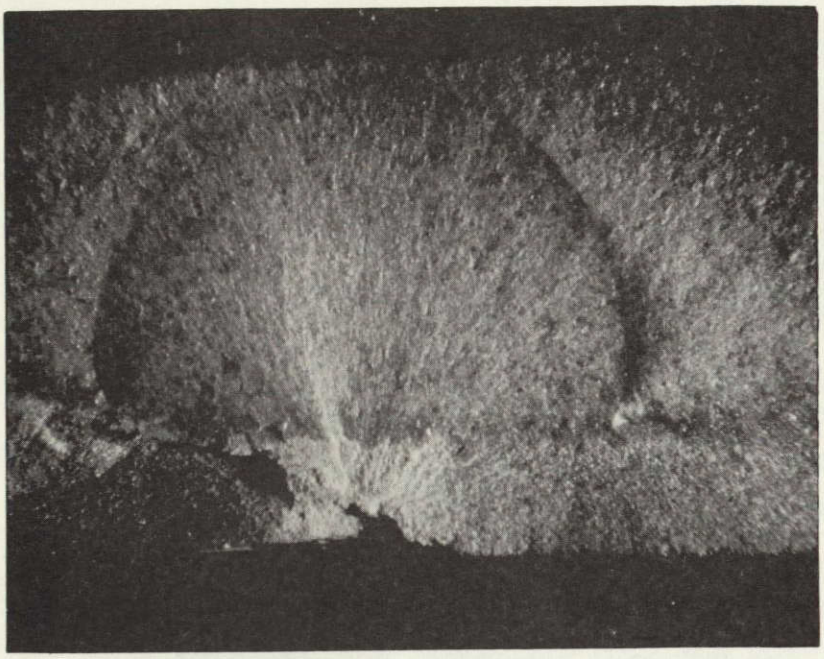

Figure 23. Fracture Surface and Damage by 1.22 J (Ballistic) Through SiC EAL on SiC Core (17.5X)

at two points 15.24 cm apart. With each firing the velocity of the pellet was readily computed from the time it took to pass over the measured distance between the two photo transistor gates. Direct readouts in microseconds were obtained for the time intervals. The range of impact energies available using the steel pellets described above varied from about 0.25 J at a velocity of 36.6 m/sec to about 8.5 J at a velocity of about 214 m/sec. At velocities higher than 214 m/sec, some instability in pellet trajectory developed.

All the test specimens were made by die-pressing and sintering techniques. They were about 5.0 cm x 5.0 cm x 1.2 cm with a center core about 7.6 mm thick and two opposing EALs each about 2.0 mm thick. Three different degrees of EAL density were obtained by varying the B content from 0% to 0.5% to 1.0% in three sets of target plates.

The results of these tests clearly showed that without a protective EAL, visible Hertzian damage was produced at ballistic impact energies of 0.29 J or less. Catastrophic damage in the form of severe cracking of the sample was produced at almost 0.67 J. On the other hand, tests on samples with EALs showed that a target specimen having 0% B in its EAL could survive an impact of

over 5.9 J without breaking. Target specimens with increasingly dense EALs survived at correspondingly lower values of impact energy. Table V shows the results of these tests.

Table V

BALLISTIC IMPACT TESTS ON SINTERED SiC
WITH AND WITHOUT EALs

	Surviving Impact Energy (J)	Fracture or Near-Fracture Impact Energy (J)
No EAL	0.29 @ 39 m/sec	0.67 @ 60 m/sec
EAL @ 1.0% B	1.16 @ 79 m/sec	1.65 @ 94 m/sec
EAL @ 0.5% B	2.10 @ 106 m/sec	3.40 @ 135 m/sec
EAL @ 0% B	5.94 @ 179 m/sec	6.63 @ 189 m/sec

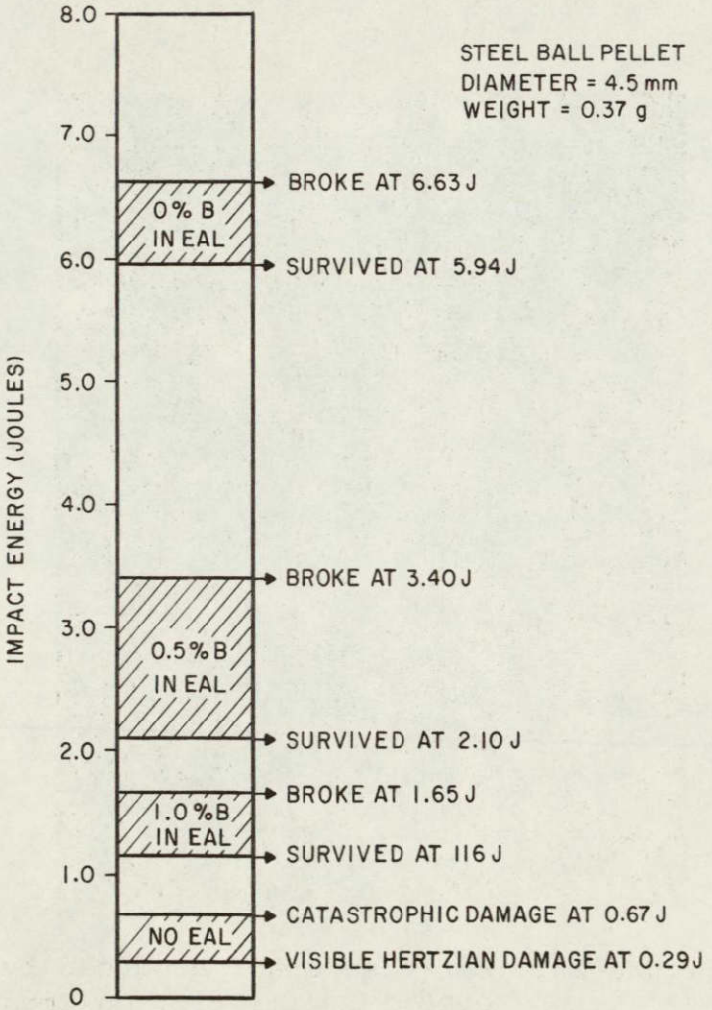

Figure 24. Ballistic Impact Tests on Sintered SiC with and without EALs

Figure 24 shows the same data presented in the form of a bar chart. These results clearly show the need for an EAL to protect the SiC from impact damage. It is also clearly observed that greater protection from catastrophic damage is afforded by the less dense EALs.

Figure 25 shows the Hertzian damage done to the surface of polished sintered SiC by an impact energy of 0.29 J imparted by the 0.37 g steel ball traveling at 39 m/sec. Surface damage to even this small degree would surely act as a low stress value crack initiator, thereby resulting in a high potential for early failure before the design stress level was imposed. Even with a ballistic impact energy as low as 0.67 J, the unprotected SiC target (5.0 cm x 5.0 cm x 9 mm) suffered catastrophic damage. Figure 26 shows the face of the plate opposite to the 0.67 J impact stress. The Hertzian ring crack produced by that shock is clearly evident.

Figure 25. Hertzian Crack Produced by 0.29 J (Ballistic) on Impact Face of Dense SiC Unprotected by EAL

Figure 26. Hertzian Ring Crack Produced by 0.67 J (Ballistic) on Face of Target Opposite to Impact Area in Dense SiC Unprotected by EAL

These initial ballistic tests indicated that porous EALs of SiC formed on SiC densified by sintering, protected the dense SiC from fracture or catastrophic failure up to impact energy levels of close to 6.0 J. However, it would seem that even at impact loadings of less than 6.0 J, some damage to the core could result if all of the energy were not absorbed in the crushing of the EAL process, or otherwise fully attenuated in the EAL. This is clearly a function of EAL density, thickness, and structure configuration. Up to this point, a single EAL on a dense core has been the only configuration examined, and it remains to be determined if less-than-catastrophic impact stress levels (6.0 J) do indeed damage the core in that configuration. Another configuration that has not been examined and could be fabricated by the same techniques would be a three-layer EAL consisting of an inner porous layer of SiC on the dense core, a dense layer and a porous

outer layer. A possible advantage of such a structure would be that any remaining impact energy unabsorbed in the outer porous layer could be spread over a large area in the next and dense SiC layer. It would then conceivably be at a subcritical stress level so as not to penetrate the inner porous layer in a concentrated area.

E. THERMAL CYCLING

To check on the uniformity of heating in the furnace it was brought up to 1350°C with the thermocouples in the same positions to be occupied by the test samples. An excellent uniformity was achieved across the six sample positions. Variations of only ±5°C were noted from one position to another.

The temperature uniformity along the length of each sample (mounted vertically) was also measured using a group of thermocouples with the couples spaced 1.27 cm apart. Starting at the base of the sample to a point 1.27 cm above the sample, the temperature varied about 25°C. The temperature on the top 4 cm of the sample varied by only about 10°C.

In additional "de-bugging" tests, two samples were run through 10 cycles in the equipment, and it was found that heating them up to 1320°C was readily accomplished in the two minute time period. It was noted that the maximum temperature did vary during the one-hour soak period at temperature. This variation was due to the additional heating required to make up for the cool air drawn into the open bottom of the furnace. Steady temperatures were realized when a gate was installed at the bottom of the furnace. It opened and closed automatically as the samples were introduced and withdrawn from the furnace.

The required sample quenching rate was not realized until additional air jets were installed and the ceramic sample holder was modified to reduce its thermal mass, and cooling air channels were cut in the holder directly beneath the samples.

Four thermal cycling test samples fabricated without EA's by techniques described in the previous section were subjected to the 100 cycle thermal cycling test procedure. The specimens were examined and weighed every 20 cycles. The results are shown in Table VI.

At the end of the 100 cycles there was no physical damage that could be found that had occurred as a result of the thermal shock stresses imposed on the specimens during the test period. Chemical interactions between the specimens surface and the combustion

Table VI

THERMAL CYCLING TESTS
SINTERED SiC - NO EALs

Specimen No.	Cycle	Weight (g)	Weight Change (g)	Weight Change (%)
92-A	0	36.435	-	-
	20	36.418	-0.017	-0.047
	40	36.418	-0.017	-0.046
	60	36.420	-0.015	-0.040
	80	36.420	-0.015	-0.041
	100	36.420	-0.015	-0.041
92-B	0	35.295	-	-
	20	35.316	+0.020	+0.051
	40	35.317	+0.021	+0.061
	60	35.319	+0.023	+0.066
	80	35.319	+0.024	+0.066
	100	35.319	+0.024	+0.066
92-C	0	36.342	-	-
	20	36.329	-0.013	-0.037
	40	36.332	-0.011	-0.030
	60	36.333	-0.010	-0.026
	80	36.333	-0.010	-0.027
	100	36.333	-0.010	-0.027
92-D	0	36.360	-	-
	20	36.339	-0.021	-0.057
	40	36.339	-0.021	-0.057
	60	36.340	-0.020	-0.054
	80	36.340	-0.020	-0.055
	100	36.340	-0.020	-0.055

products were minimal. Weight losses remained essentially constant for each specimen after the 20th cycle. The small weight losses experienced by samples 92-A, -C, and -D were probably due to a small amount of gas erosion that took place. Another possible weight loss, or gain (as noted in sample 92-B) explanation could be found in the differences in flame chemistry. Reducing and oxidizing atmospheres could produce different results in the weight changes as noted.

The results of thermal cycling tests on test wedges with SiC EALs are shown in Table VII. These were fabricated according to the procedure described in the previous section of this report. Three samples were made and tested. Each sample was made with a different amount of EAL on the specimen. Sample numbers 106-A, -B, and -C had EALs weighing 0.628 g, 1.034 g, and 1.218 g, respectively.

Table VII

THERMAL CYCLING TESTS
SINTERED SiC - WITH EALs

Specimen	Cycle	Weight (g)	Weight Change (g)	Weight Change as a Percentage of Total Sample Weight	Weight Change as a Percentage of EAL Weight
102-A	0	37.947	-	-	-
(Est. EAL	20	38.093	+0.146	+0.385	+23.2
wt = 0.629 g)	40	38.128	+0.182	+0.479	+28.9
	60	38.131	+0.184	+0.486	+29.3
	80	38.165	+0.218	+0.576	+34.7
	100	38.172	+0.226	+0.595	+35.9
102-B	0	38.585	-	-	-
(Est. EAL	20	38.799	+0.214	+0.554	+20.7
wt = 1.034 g)	40	38.850	+0.275	+0.712	+26.6
	60	38.900	+0.314	+0.814	+30.4
	80	38.930	+0.345	+0.895	+33.4
	100	38.964	+0.379	+0.982	+36.6
102-C	0	38.575	-	-	-
(Est. EAL	20	38.762	+0.187	+0.484	+15.3
wt = 1.218 g)	40	38.812	+0.237	+0.613	+19.4
	60	38.841	+0.266	+0.689	+21.8
	80	38.863	+0.288	+0.745	+23.6
	100	38.868	+0.293	+0.759	+24.0

The final inspection of the three specimens after completion of the 100-cycle test revealed no evidence of thermal shock damage to either the EAL or the core body. Figure 27 is a photograph of specimen No. 106-A taken after the 100-cycle thermal cycling test. Flaws in the EAL such as the pinholes and small bumps apparent in the photograph, and present in the EAL to begin with, were not exaggerated or made worse in any way by the thermal cycling program. The porous nature of the EALs is revealed in the weight gains experienced by the samples. If the weight gains represent the surface oxidation of the pore channels in the EAL to silica, the weight gains made by samples 102-A and 102-B indicate that close to 24% of the SiC in the EAL was oxidized to SiO_2. On a similar basis, the EAL on test piece 102-C had only 15% of its EAL converted to SiO_2. This could be due to nonuniform atmosphere zones in the furnace. It is conceivable that the one test piece was exposed to less oxidative combustion gas products than the other two specimens.

Figures 28 and 29 are photomicrographs of the as-polished microstructures of a thermal cycle test wedge having an EAL taken after the 100-cycle test. Figure 28 shows the microstructure of the core material and Figure 29 shows the interfacial zone between the core and the porous EAL. There were no apparent structure changes generated in the core material as a result of the thermal cycling. A full field view of the EAL structure of the same test piece is shown in Figure 30. The composite structure of densified SiC and porosity is clearly revealed. The curled filaments of SiC shown in Figure 30 are typical of the SiC powder used to form the EALs in this program.

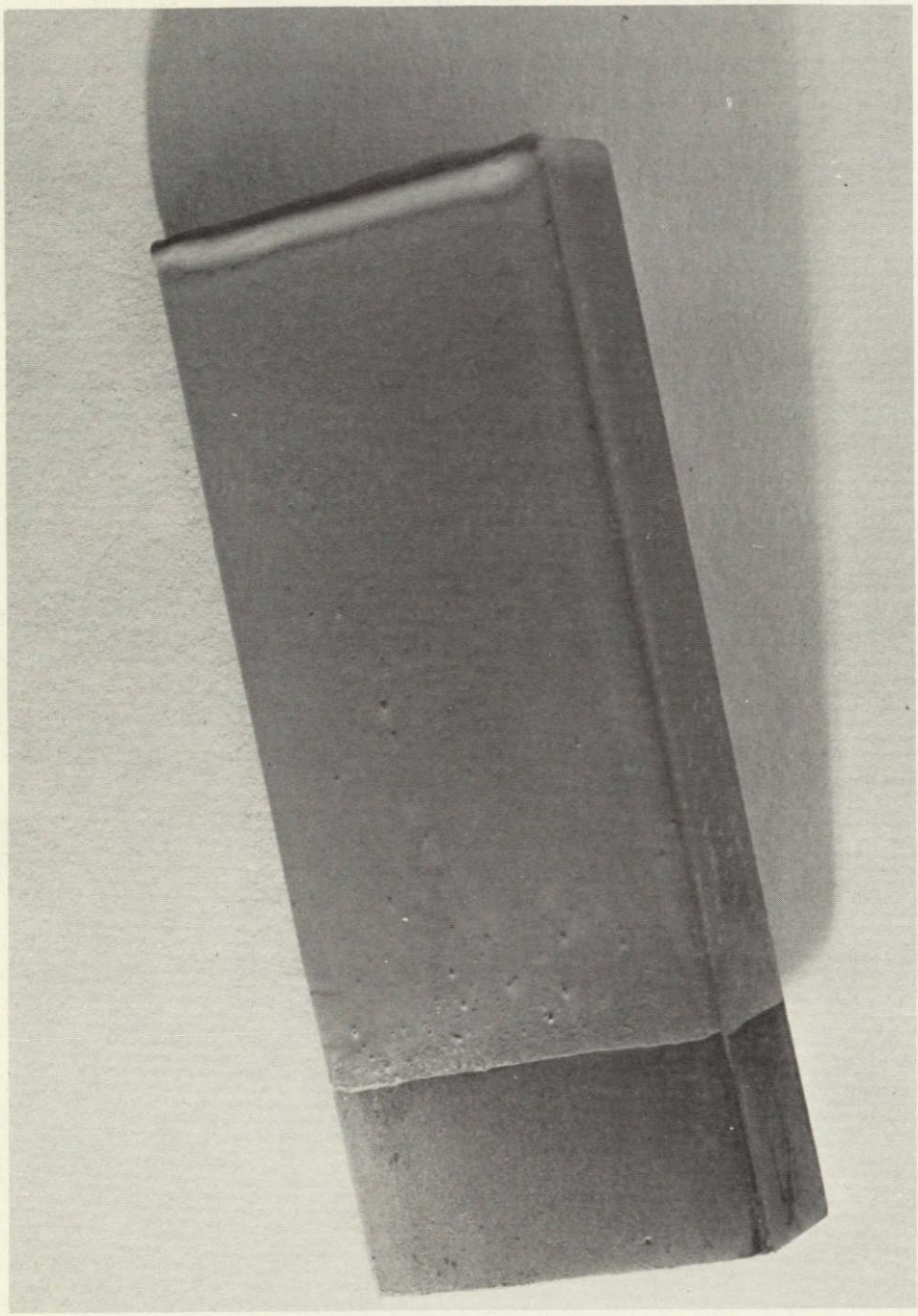

Figure 27. Thermal Cycle Test Wedge No. 106-A
Taken After 100 Cycles (2.5X)

Figure 28. Microstructure of Core Material of Thermal Cycle Test Wedge After 100 Cycles (300X)

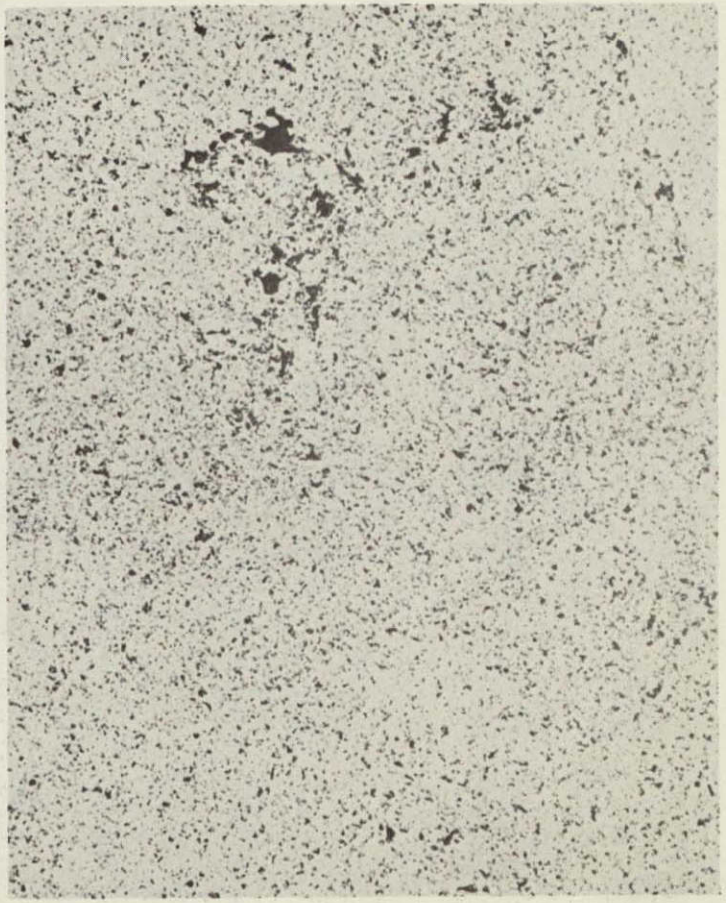

Figure 29. Microstructure of Interfacial Zone Between the Core and Porous EAL in Thermal Cycle Test Wedge After 100 Cycles (300X)

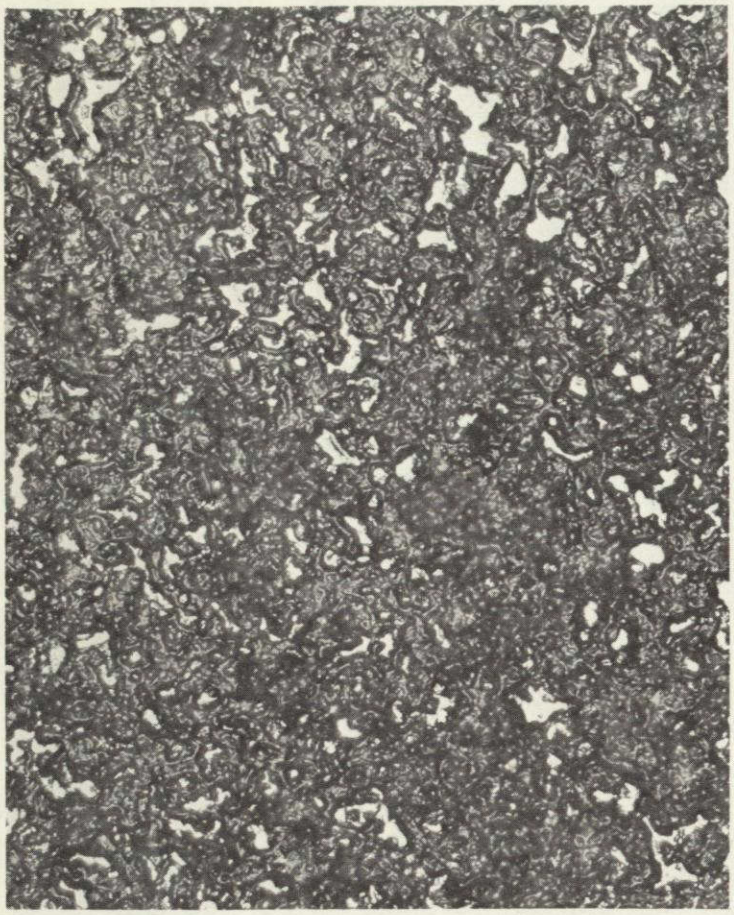

Figure 30. Full Field of EAL Microstructure in Thermal Cycle Test Wedge After 100 Cycles

(300X)

V. SUMMARY OF RESULTS

1. Two processes were developed for producing SiC components equipped with porous SiC energy absorbing layers.

2. No degradation in strength of the dense load-bearing core occurred as a result of the processing required to fabricate the SiC structures equipped with the SiC EALs.

3. No degradation in strength of EAL equipped SiC occurred when tested at 1325°C as compared with the room temperature values.

4. The fracture strength of test bars with EALs containing no added boron was significantly higher at 1325°C than at room temperature.

5. Increasing levels of boron doping in the EALs resulted in small changes in strength, with no significant trends observed, from the limited number of tests made at room temperature and at 1325°C.

6. A very narrow scatter band was found in the results of any one set of bend strength tests at both room temperature and at 1325°C.

7. There was a wide scatter within certain groups of samples in the results of the Charpy impact tests, however, little if any differences were noted between the room temperature and 1325°C Charpy impact-test results.

8. No catastrophic failures such as spalling, cracking or fracture occurred when material specimens with EALs were subjected to thermal cycling between room temperature and 1325°C.

9. Ballistic impact tests indicated that porous SiC EALs can protect a SiC substrate from breaking up in catastrophic failure at energy levels approaching 6.0 J.

VI. CONCLUSIONS

In previous attempts to apply porous energy absorbing layers (EALs) onto surfaces of already fully densified SiC, it was found that the processes required to apply the surface layer also caused an unacceptable weakening of the base SiC. As a result of this investigation, two processes were developed for producing SiC components equipped with porous SiC energy absorbing layers. From the experimental data obtained, it was determined that the processing steps used in fabricating such structures did not weaken the dense load-bearing member of the structure. Tests showed that there was no difference in bend strength between test bars having two EALs and those that were made with two EALs but tested in three-point flexure with one EAL ground off, and with the ground-off face in tension during the test.

A general, but nevertheless important conclusion drawn from the results of this work is that the dip-coating process developed for applying the SiC EALs to the thermal cycling test wedges and the erosion test bars offers promise that complex geometrical shapes of dense SiC can be economically equipped with porous SiC layers.

Three-point bend tests were used to determine modulus of rupture values for dense SiC equipped with EALs of varying densities at room temperature and at 1325°C. The results of these tests indicated that there was essentially no degradation in strength at 1325°C of EAL-equipped SiC as compared with the room-temperature values. The fracture strength of test bars with EALs containing no added boron increased significantly at 1325°C as compared to their strength at room temperature. The opposite observation was noted when boron was added to the EAL. Increasing levels of boron doping in the EAL resulted in decreasing strengths at room temperature and at 1325°C. These results led to the conclusion that for maximum strength in the EAL equipped structure, the boron doping in the EAL must be kept low, preferably at zero.

The quite narrow scatter band in the results of any one set of bend strength tests suggested that the scatter in flaw size had been narrowed, resulting in a more uniform strength from bar to bar.

The wide scatter in the Charpy impact results within certain groups of these tests was disappointing, particularly in view of the very consistent results obtained in the bend strength determinations. Room temperature and 1325°C Charpy tests indicated

little if any differences due directly to the test temperature and its attendant environment. The average Charpy values in terms of elastic energy stored per unit volume indicated no significant increases were obtained with specimens equipped with boron-doped EALs as compared to samples having no EALs.

Thermal cycling test wedges with an without EALs showed that both forms of structures were highly resistant to both thermal shock and to oxidation. No catastrophic failures such as spalling or cracking occurred during any of the thermal cycling tests.

From some preliminary ballistic tests conducted on specimens with and without EALs, it was concluded that without an EAL to protect it, a SiC body will suffer surface damage from ballistic impact energies as low as 0.29 J. At impact energies of only 0.67 J the same body was catastrophically damaged, and rendered useless. Equipped with a porous SiC EAL applied over the dense load-bearing SiC the body withstood catastrophic failure from ballistic impact energies approaching 6.0 J.

VII. REFERENCES

1. T.R. Wright and D.E. Niesz, Improved Toughness of Refractory Compounds, Battelle Columbus Laboratories Report, NASA CR-134690, Contract NAS3-17766, Colombus, Ohio, October 1974.

2. H.P. Kirchner and J. Seretsky, Improving Impact Resistance of Ceramic Materials by Energy Absorbing Surface Layers, Ceramic Finishing Company Report, NASA CR-134644, Contract NAS3-17765, March 1974.

3. R.M. Cannon, Jr. and R.J. Hill, High Temperature Compounds for Turbine Vanes, Avco Corporation Report, NASA CR-72794, Contract NAS3-13213, August 1970.

4. D.R. Platts, H.P. Kirchner and R.M. Graver, Strengthening Oxidation Resistant Materials for Gas Turbine Applications, Ceramic Finishing Company Summary Report, NASA CR-121002, Contract NAS3-15561, September 1972.

5. J.A. Palm, Improved Toughness of Refractory Compounds, General Electric Company Report, NASA CR-134921, Contract NAS3-17767, General Electric Corporate Research and Development, Schenectady, N.Y., November 1975.

6. S. Prochazka, "Sintering of Silicon Carbide," Ceramics for High Performance Applications, Proceedings of the Second Army Materials Technology Conference, John J. Burke, Alvin E. Greene and R. Nathan Katz, eds., 1974, pp. 239-252.